transcription of *FKBP5* through the intronic sequence we identified rather than a promoter sequence.

The DNA sequences that were responsive to DEX in our study were aligned in Figure 5b. The recognition sequence of GR is defined as a 15-bp motif with partial dyad symmetry such as 5′-GGTACAnnnTGTTCT-3′.[31] However, a mutagenesis study indicated that some sequences that do not perfectly fit into the consensus sequence are still GC-responsive.[30] Based on our results, three repeats of 5′-WGWWCW-3′ separated by 1–4 bp are responsive to GC in which the second motif needs to have a perfect match. However, the presence of this sequence alone does not result in a functional GRE. Indeed, the sequence in *GZMA* that fulfills this consensus sequence, for example GRE2 in Figure 3c, was not functional, because disruption of this candidate GRE had little effect on the response to GC. Therefore, the induction potential of a given site is speculated to be a complex function in the context of the higher gene structure.

The molecular mechanism of GC-induced apoptosis is not fully understood. In the first place, it is necessary for GR to function as a transactivator in order to induce apoptosis, because mutant GR incapable of binding DNA fails to induce thymocyte apoptosis[32] and inhibition of *de novo* protein synthesis by CHX virtually eliminated DEX-induced apoptosis in 697 cells (data not shown). In addition to the genes investigated in this study, the *Bim* gene (*BCL2L11*) has recently been reported to be induced by GC in murine lymphoma cell lines.[25] Bim protein is a BH3-only member of the Bcl-2 family that is capable of directly activating the apoptotic cascade.[33] It is therefore an attractive candidate for a GC target gene that mediates apoptosis. However, at least in our microarray analysis, *Bim* expression was not induced at any time points examined after DEX treatment, although its expression at low levels was observed (data not shown). Thus, we conclude that *Bim* is unlikely a target of GC that generally mediates GC-induced apoptosis. Nevertheless, the levels of *Bim* expression may determine the sensitivity of leukemic cells to GC, since GC-induced apoptosis is partially impaired in hematopoietic cells from $Bim^{-/-}$ mice.[34]

Is one of the genes investigated here solely responsible for GC-induced cell death? We established a lentivirus-mediated small interference RNA delivery system to selectively knock down *FKBP5* or *DSCR1*. The knocking-down of a single gene, however, was not sufficient to significantly inhibit GC-induced apoptosis, suggesting that multiple GR-induced genes activate a network of pathways that contribute to apoptosis (data not shown). This is reminiscent of p53-induced apoptosis. More than 16 target genes of p53 have been proposed to mediate apoptosis, but it is still unclear whether any single target gene is critical. Several lines of evidence suggest that the signaling pathway of p53-induced apoptosis is cell type-dependent and two or more genes cooperate to induce cell death in certain situations.[35,36] In this regard, it should be noted that the *granzyme K* gene, *GZMK*, is also significantly upregulated by GC (data not shown). *GZMK* encodes a serine protease that has features common to granzyme A, and the two genes are only ~70 kb apart on human chromosome 5. Thus, *GZMK* may be another target of GC that mediates apoptosis. Generating mice doubly deficient in GC target genes would help to clarify the signal transduction of GC-induced apoptosis. Expression profiling of the genes described in this study will contribute to predictions of responsiveness or resistance to GC therapy. Further study of GC target genes will provide the rationale for the optimal use of GC to improve treatment outcome in leukemia.

Acknowledgements

We thank Kaori Inoue and Mayu Yamazaki for technical support, Kayoko Saito for preparing the manuscript, and Dr Keith Yamamoto for providing plasmids. This work was supported by Grants for Cancer Research, Genome Research and Child Health and Development from the Ministry of Health, Labour and Welfare; Grant-in-Aid for Scientific Research and the Budget for Nuclear Research from the Ministry of Education, Culture, Sports, Science and Technology, Japan.

Supplementary Information

Supplementary Information accompanies the paper on the Leukemia website (http://www.nature.com/leu).

References

1 Distelhorst CW. Recent insights into the mechanism of glucocorticosteroid-induced apoptosis. *Cell Death Differ* 2002; **9**: 6–19.
2 Tissing WJ, Meijerink JP, den Boer ML, Pieters R. Molecular determinants of glucocorticoid sensitivity and resistance in acute lymphoblastic leukemia. *Leukemia* 2003; **17**: 17–25.
3 Riccardi C, Cifone MG, Migliorati G. Glucocorticoid hormone-induced modulation of gene expression and regulation of T-cell death: role of GITR and GILZ, two dexamethasone-induced genes. *Cell Death Differ* 1999; **6**: 1182–1189.
4 Barker PE, Carroll AJ, Cooper MD. t(1;19)(q23;p13) in pre-B acute lymphocytic leukemia cell line 697. *Cancer Genet Cytogenet* 1987; **25**: 379–380.
5 Yoshida N-L, Miyashita T, U M, Yamada M, Reed JC, Sugita Y *et al*. Analysis of gene expression patterns during glucocorticoid-induced apoptosis using oligonucleotide arrays. *Biochem Biophys Res Commun* 2002; **293**: 1254–1261.
6 Beresford PJ, Kam CM, Powers JC, Lieberman J. Recombinant human granzyme A binds to two putative HLA-associated proteins and cleaves one of them. *Proc Natl Acad Sci USA* 1997; **94**: 9285–9290.
7 Shresta S, Graubert TA, Thomas DA, Raptis SZ, Ley TJ. Granzyme A initiates an alternative pathway for granule-mediated apoptosis. *Immunity* 1999; **10**: 595–605.
8 Fuentes JJ, Pritchard MA, Estivill X. Genomic organization, alternative splicing, and expression patterns of the *DSCR1* (Down syndrome candidate region 1) gene. *Genomics* 1997; **44**: 358–361.
9 Baughman G, Wiederrecht GJ, Campbell NF, Martin MM, Bourgeois S. FKBP51, a novel T-cell-specific immunophilin capable of calcineurin inhibition. *Mol Cell Biol* 1995; **15**: 4395–4402.
10 Vega RB, Yang J, Rothermel BA, Bassel-Duby R, Williams RS. Multiple domains of MCIP1 contribute to inhibition of calcineurin activity. *J Biol Chem* 2002; **277**: 30401–30407.
11 Yamada M, Hirasawa A, Shiojima S, Tsujimoto G. Granzyme A mediates glucocorticoid-induced apoptosis in leukemia cells. *FASEB J* 2003; **17**: 1712–1714.
12 Zhao Y, Tozawa Y, Iseki R, Mukai M, Iwata M. Calcineurin activation protects T cells from glucocorticoid-induced apoptosis. *J Immunol* 1995; **154**: 6346–6354.
13 Asada A, Zhao Y, Kondo S, Iwata M. Induction of thymocyte apoptosis by Ca^{2+}-independent protein kinase C (nPKC) activation and its regulation by calcineurin activation. *J Biol Chem* 1998; **273**: 28392–28398.
14 McEwan IJ, Wright AP, Gustafsson JA. Mechanism of gene expression by the glucocorticoid receptor: role of protein–protein interactions. *BioEssays* 1997; **19**: 153–160.
15 Stöcklin E, Wissler M, Gouilleux F, Groner B. Functional interactions between Stat5 and the glucocorticoid receptor. *Nature* 1996; **383**: 726–728.
16 Imai Y, Matsushima Y, Sugimura T, Terada M. A simple and rapid method for generating a deletion by PCR. *Nucleic Acids Res* 1991; **19**: 2785.

17 Pawlowski V, Revillion F, Hornez L, Peyrat JP. A real-time one-step reverse transcriptase-polymerase chain reaction method to quantify c-erbB-2 expression in human breast cancer. *Cancer Detect Prev* 2000; **24**: 212–223.
18 Miesfeld R, Rusconi S, Godowski PJ, Maler BA, Okret S, Wikstrom AC *et al.* Genetic complementation of a glucocorticoid receptor deficiency by expression of cloned receptor cDNA. *Cell* 1986; **46**: 389–399.
19 Shikama Y, Yamada M, Miyashita T. Caspase-8 and caspase-10 activate NF-κB through RIP, NIK and IKKα kinases. *Eur J Immunol* 2003; **33**: 1998–2006.
20 Galon J, Franchimont D, Hiroi N, Frey G, Boettner A, Ehrhart-Bornstein M *et al.* Gene profiling reveals unknown enhancing and suppressive actions of glucocorticoids on immune cells. *FASEB J* 2002; **16**: 61–71.
21 Planey SL, Abrams MT, Robertson NM, Litwack G. Role of apical caspases and glucocorticoid-regulated genes in glucocorticoid-induced apoptosis of pre-B leukemic cells. *Cancer Res* 2003; **63**: 172–178.
22 Tonko M, Ausserlechner MJ, Bernhard D, Helmberg A, Kofler R. Gene expression profiles of proliferating *vs* G1/G0 arrested human leukemia cells suggest a mechanism for glucocorticoid-induced apoptosis. *FASEB J* 2001; **15**: 693–699.
23 Chauhan D, Auclair D, Robinson EK, Hideshima T, Li G, Podar K *et al.* Identification of genes regulated by dexamethasone in multiple myeloma cells using oligonucleotide arrays. *Oncogene* 2002; **21**: 1346–1358.
24 Yang J, Rothermel B, Vega RB, Frey N, McKinsey TA, Olson EN *et al.* Independent signals control expression of the calcineurin inhibitory proteins MCIP1 and MCIP2 in striated muscles. *Circ Res* 2000; **87**: E61–E68.
25 Wang Z, Malone MH, He H, McColl KS, Distelhorst CW. Microarray analysis uncovers the induction of the proapoptotic BH3-only protein Bim in multiple models of glucocorticoid-induced apoptosis. *J Biol Chem* 2003; **278**: 23861–23867.
26 Kastan MB, Zhan Q, el Deiry WS, Carrier F, Jacks T, Walsh WV *et al.* A mammalian cell cycle checkpoint pathway utilizing p53 and *GADD45* is defective in ataxia-telangiectasia. *Cell* 1992; **71**: 587–597.
27 Oda K, Arakawa H, Tanaka T, Matsuda K, Tanikawa C, Mori T *et al. p53AIP1*, a potential mediator of p53-dependent apoptosis, and its regulation by Ser-46-phosphorylated p53. *Cell* 2000; **102**: 849–862.
28 de Stanchina E, Querido E, Narita M, Davuluri RV, Pandolfi PP, Ferbeyre G *et al.* PML is a direct p53 target that modulates p53 effector functions. *Mol Cell* 2004; **13**: 523–535.
29 Hubler TR, Denny WB, Valentine DL, Cheung-Flynn J, Smith DF, Scammell JG. The FK506-binding immunophilin FKBP51 is transcriptionally regulated by progestin and attenuates progestin responsiveness. *Endocrinology* 2003; **144**: 2380–2387.
30 Strähle U, Klock G, Schütz G. A DNA sequence of 15 base pairs is sufficient to mediate both glucocorticoid and progesterone induction of gene expression. *Proc Natl Acad Sci USA* 1987; **84**: 7871–7875.
31 Beato M, Chalepakis G, Schauer M, Slater EP. DNA regulatory elements for steroid hormones. *J Steroid Biochem* 1989; **32**: 737–747.
32 Reichardt HM, Kaestner KH, Tuckermann J, Kretz O, Wessely O, Bock R *et al.* DNA binding of the glucocorticoid receptor is not essential for survival. *Cell* 1998; **93**: 531–541.
33 O'Connor L, Strasser A, O'Reilly LA, Hausmann G, Adams JM, Cory S *et al.* Bim: a novel member of the Bcl-2 family that promotes apoptosis. *EMBO J* 1998; **17**: 384–395.
34 Bouillet P, Metcalf D, Huang DC, Tarlinton DM, Kay TW, Kontgen F *et al.* Proapoptotic Bcl-2 relative Bim required for certain apoptotic responses, leukocyte homeostasis, and to preclude autoimmunity. *Science* 1999; **286**: 1735–1738.
35 Lindsten T, Ross AJ, King A, Zong WX, Rathmell JC, Shiels HA *et al.* The combined functions of proapoptotic Bcl-2 family members bak and bax are essential for normal development of multiple tissues. *Mol Cell* 2000; **6**: 1389–1399.
36 Villunger A, Michalak EM, Coultas L, Müllauer F, Böck G, Ausserlechner MJ *et al.* p53- and drug-induced apoptotic responses mediated by BH3-only proteins puma and noxa. *Science* 2003; **302**: 1036–1038.

Purification, Molecular Cloning, and Expression of a Novel Growth-Promoting Factor for Retinal Pigment Epithelial Cells, REF-1/TFPI-2

Yasuhiko Tanaka,[1] Jun Utsumi,[2] Mizuo Matsui,[3] Tetsuo Sudo,[2] Noriko Nakamura,[2] Masato Mutoh,[2] Akemi Kajita,[2] Saburo Sone,[2] Kazuteru Kigasawa,[4] Masahiko Shibuya,[1] Venkat N. Reddy,[5] Qiang Zhang,[1,6] and Takeshi Iwata[1]

PURPOSE. Retinal pigment epithelial (RPE) cells are known to play important roles in maintaining the homeostasis of the retina and in controlling choroidal neovascularization. The purpose of this study was to identify a factor or factors that would stimulate RPE cells to proliferate.

METHODS. To isolate such a factor, 100 L of human-fibroblast-conditioned medium underwent ion-exchange, hydrophobic, and reverse-phase chromatographies followed by sodium dodecyl sulfate–polyacrylamide gel electrophoresis. The growth-promoting activity of the factor was examined in a human K-1034 RPE cell line and human primary RPE cells.

RESULTS. The different chromatographic processes isolated a 31-kDa factor that had RPE cell growth–promoting properties. This factor, which we have named RPE cell factor (REF)-1, promotes growth of RPE cells but not of human umbilical vein endothelial cells (HUVECs). The amino-terminal sequence and molecular cloned cDNA of REF-1 were identical with those of tissue-factor pathway inhibitor (TFPI)-2, a family of TFPIs, and placental protein (PP)-5, a serine protease inhibitor. The cDNA expression of REF-1/TFPI-2 with pcDL-pSRα vector in Chinese hamster ovary (CHO) cells confirmed the growth-promoting activity for RPE cells. The major component of the recombinant REF-1/TFPI-2 expressed in CHO cells had a molecular mass of 31 kDa and exerted growth-promoting activity in RPE cells but not in human endothelial cells and fibroblasts in vitro. REF-1/TFPI-2 also had protease inhibitory activity. The other family factor, TFPI-1, did not promote RPE cell growth.

CONCLUSIONS. REF-1/TFPI-2 is a novel growth-promoting factor for RPE cells but not for endothelial cells and fibroblasts. Its properties make it potentially beneficial for intraocular therapy for the repair and maintenance of RPE cells. (*Invest Ophthalmol Vis Sci.* 2004;45:245–252) DOI:10.1167/iovs.03-0230

Recent advances in basic and clinical research have shown that the pathogenesis of many retinal and choroidal diseases is closely related to the normal functioning of retinal pigment epithelial (RPE) cells. RPE cells play critical roles in maintaining the homeostasis of the retina and in controlling choroidal neovascularization.[1] Because the denaturation of cellular proteins in the RPE and the loss of function of RPE cells are responsible for retinal and choroidal diseases, a factor that stimulates RPE cell growth could prove to be valuable for the treatment of RPE-related ocular diseases.

At present, various cell growth factors, such as basic fibroblast growth factor (bFGF) and platelet-derived growth factor (PDGF), are known to stimulate the proliferation of RPE cells.[2–4] However, these factors are also known to affect the growth of vascular endothelial cells and fibroblasts,[5–7] and ocular neovascularization and fibroblast proliferation can lead to serious retinal and choroidal diseases and proliferative vitreoretinopathy.

The purpose of this study was to isolate and characterize a factor or factors that would promote RPE cell proliferation. We focused on the supernatant of cultured human fibroblasts as a source of the target factor, because fibroblasts function as stromal cells that are known to produce various cytokines. We have isolated a 31-kDa factor from the conditioned medium of human fibroblasts that promotes growth in RPE cells and named it RPE cell factor (REF)-1. The amino terminal sequence was determined, and molecular cloning of its cDNA showed that the factor was identical with tissue-factor pathway inhibitor (TFPI)-2[8]-placental protein 5 (PP5).[9]

MATERIALS AND METHODS

Isolation of RPE Cell Growth–Promoting Factor

Human fibroblast DIP-2 cells[10] were cultured for 5 days in Eagle's minimum essential medium (MEM) supplemented with 5% fetal calf serum (FCS) in microcarriers (Cytodex 1; Amersham Biosciences, Tokyo, Japan) in 16-L glass culture vessels at 37°C. After the addition of 100 IU/mL human interferon-β (Toray Industries, Tokyo, Japan) as a priming agent and 10 μg/mL poly(I) poly(C) (Yamasa Shouyu, Choushi, Japan) as a cytokine-inducing reagent, the culture media was replaced by serum-free Eagle's MEM and cultured at 37°C for six additional days.

The cultured medium was collected and filtered to remove the cellular debris. Fractionation was started by passing 100 L of the cultured medium through an S-Sepharose column (500 mL; Amersham Biosciences), and the fraction containing growth-promoting activity (active fraction) was eluted with 200 mL of 10 mM phosphate-buffered

From the [1]National Institute of Sensory Organs, National Tokyo Medical Center, Tokyo, Japan; the [2]Pharmaceutical Research Laboratories, Toray Industries, Inc., Kamakura, Japan; the [3]Department of Ophthalmology, Nihon University Surugadai Hospital, Tokyo, Japan; the [4]Department of Ophthalmology, Tokai University School of Medicine, Isehara, Japan; the [5]Department of Ophthalmology, Kellogg Eye Center, University of Michigan, Ann Arbor, Michigan; and the [6]Department of Ophthalmology, Keio University School of Medicine, Tokyo, Japan.

Supported in part by grants for Research on Sensory and Communicative Disorders by the Ministry of Health, Labor and Welfare, Japan and by National Eye Institute Grants EY00484 and EY07003.

Submitted for publication March 5, 2003; revised September 1, 2003; accepted September 4, 2003.

Disclosure: **Y. Tanaka**, None; **J. Utsumi**, Toray Industries (F, E, P); **M. Matsui**, None; **T. Sudo**, Toray Industries (F, E); **N. Nakamura**, Toray Industries (F, E); **M. Mutoh**, Toray Industries (F, C, P); **A. Kajita**, Toray Industries (F, E); **S. Sone**, Toray Industries (F, E); **K. Kigasawa**, None; **M. Shibuya**, None; **V.N. Reddy**, None; **Q. Zhang**, None; **T. Iwata**, None

The publication costs of this article were defrayed in part by page charge payment. This article must therefore be marked "*advertisement*" in accordance with 18 U.S.C. §1734 solely to indicate this fact.

Corresponding author: Yasuhiko Tanaka, National Institute of Sensory Organs, National Tokyo Medical Center, 2-5-1 Higashigaoka, Meguro-ku, Tokyo 152-8902, Japan; ytanaka@ntmc.hosp.go.jp.

saline (PBS) at pH 7.4 with 0.5 M NaCl. The eluate was added to 1 M ammonium sulfate and applied to a polypropyl A column (0.8 × 25 cm; PolyLC, Columbia, MD). The active protein was eluted by a gradient of 0 to 1 M ammonium sulfate in 10 mM PBS. Four milliliters of the active fraction from the polypropyl A column were injected into a C4 reverse-phase column (1 × 25 cm; Grace Vydac, Hesperia, CA), and the protein was eluted by a gradient of water-acetonitrile (0%–70%) including 0.1% trifluoroacetic acid (TFA; pH 2.0). Two milliliters of the active fraction eluted from the column was concentrated to 100 μL by speed vacuum concentrator (Speed Vac Systems, Savant, MN) and applied to sodium dodecyl sulfate-polyacrylamide gel electrophoresis (SDS-PAGE) under nonreducing conditions without 2-mercaptoethanol (2ME). Immediately after migration of the sample into the gel, the SDS-PAGE gel was cut into 1 × 2 × 4-mm slices and immersed overnight at 4°C in 0.5 mL per slice of distilled water to extract the active protein. The extracted protein was reapplied to SDS-PAGE under reducing–nonreducing conditions to examine the purity and the molecular weight of the target protein.

Determination of Cell Growth–Promoting Activity during Purification

Human K-1034 RPE cells or fourth-passage human primary RPE cells were used to determine RPE cell growth-promoting activity.[11] K-1034 cells or human primary RPE cells were added to collagen type I-coated 24-well plastic plates (Corning International, Tokyo, Japan) at a density of 1×10^4 cells/well. DMEM supplemented with 5% FCS (Invitrogen Japan, Tokyo, Japan) or 15% FCS (Invitrogen) was used for K-1034 or human primary RPE cells, respectively. Two microliters of purified REF-1 was added to each well and cultured at 37°C for 5 days. The number of RPE cells at each time point was determined by a cell counter (model ZM; Beckman Coulter K. K., Tokyo, Japan). The growth-promoting rate was calculated as a percentage of the control ($n = 4$ or 6). In the first exploratory purification, the specific concentration of REF-1 was not determined, as an REF-1 ELISA kit is not available, and REF-1 was therefore traced by the growth-promoting activity in RPE cells.

Determination of Cell Growth–Promoting Activity Using Purified REF-1 Protein

To examine whether purified REF-1 promotes growth in the number of vascular endothelial cells, cells were isolated from the human umbilical vein of a patient at an obstetric hospital. In accordance with the provisions of the Declaration of Helsinki, all subjects signed an informed consent after an explanation of the procedures to be used and the purpose of the studies. The human umbilical vein endothelial cells (HUVECs) were treated under conditions similar to those used for RPE cells ($n = 4$ or 6). Human fibroblasts (DIP-2 cells), rabbit primary RPE cells, and human primary RPE cells were also used to characterize the growth-promoting activity ($n = 6$).

A comparison of the growth-promoting profile of other related factors, such as TFPI-1 (American Diagnostica, Greenwich, CT), the family of TFPIs, ciliary neurotrophic factor (CNTF; R&D Systems, Minneapolis, MN), and bFGF (R&D Systems), was performed at a concentration of 10 ng/mL ($n = 6$).

Amino Acid Analyses of REF-1/TFPI-2

REF-1 was isolated as a 31 ± 3-kDa protein on SDS-PAGE gel under nonreducing conditions. The active fraction appeared to correspond to a single band on the silver-stained gel. REF-1 was isolated from the band and subjected to amino-terminal amino acid sequence analysis (Protein sequencer model 470; Applied Biosystems Japan, Tokyo, Japan).

Amino acid composition analysis of REF-1 component was performed after hydrolysis at 110°C for 22 and 72 hours in 6 M HCl with 4% thioglycolic acid (amino acid analyzer model 835; Hitachi, Tokyo, Japan).

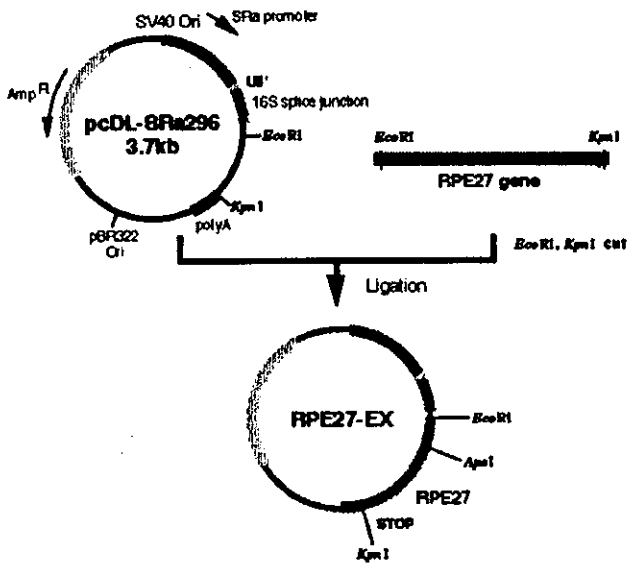

FIGURE 1. The construction of the REF-1 expression vector. The RPE27-EX1 expression vector was obtained by ligation with pcDL-SRα296 vector (3.7 kb) and RPE27 gene (750 bp).

Molecular Cloning of REF-1 Protein

The primers, R1: 5′-GGAAGAAGGCACATGGC-3′, R2: 5′-TATGGGGATTGGTGGCG-3′, R3: 5′-ACTCCTGGAGCCCGTC-3′, L1: 5′-AGACATGGCCTGCCCG-3′, L2: 5′-GACACCAGACCAACTGG-3′, and L3: 5′-GGTAGCGACCGGCGC-3′ were used for PCR amplification of phage insert and were designed based on the sequence of cloning vector λgt11 (Human placenta cDNA library, CLHL1008b; BD Biosciences-Clontech Japan, Tokyo, Japan). The first PCR was performed with primers, R1 and L1, designed to flank the insert of λgt11. The second PCR was performed using 1 μL of the first PCR reaction mixture as template with three primers: 27S1 (5′-GATGCIGAACAAGAACCIACIG-3′) and the R2 and L2 primers. The third PCR was performed with the second PCR mixture as a template, with primer 27S2 (5′-CAAGAACCIACIG-GIACIAATGC-3′) and the R3 and L3 primers.

The PCR conditions were initiated at 94°C for 5 minutes, then 25 cycles at 94°C for 30 seconds, 56°C for 2 minutes, and 72°C for 8 minutes, followed by 1 cycle at 72°C for 7 minutes. The amplified DNA fragment from the third PCR was separated by 1% agarose gel electrophoresis and the DNA fragment was purified from gel by the electroelution method. Purified DNA fragment was cloned using a kit (Sure Clone; Amersham Bioscience). The nucleotide sequence was determined for 16 clones containing full-length cDNA on a DNA sequencer (model 373A; Applied Biosystems).

Construction of Expression Vector for REF-1/TFPI-2

REF-1 cDNA was reamplified by PCR from an original λgt11 phage clone by primer set RPE27-EX1 (5′-GGGGAATTCCTTTCTCGGACGGCTTGC-3′) and RPE27-EX2 (5′-GGGGGTACCTAAAAATTGCTTCTTCCG-3′) to obtain the insert for the expression vector. PCR was performed for 25 cycles in a reaction mixture with 0.2 μg of λgt11 DNA, 1.6 mM dNTP, 1.0 μM of primers (RPE 27-EX1 and RPE 27-EX2), and DNA polymerase (Ex *Taq*; Takara, Tokyo, Japan). The PCR product was digested with *Eco*RI and *Kpn*I and ligated into expression vector pcDL-SRα296 to obtain expression vector RPE27-EX (Fig. 1).[12]

Expression of Recombinant REF-1/TFPI-2 by CHO Cells

The expression vector RPE27-EX and the expression vector pAdDHFR containing dihydrofolate reductase (DHFR) cDNA were cotransfected

into the DHFR gene-deficient CHO DXB11 cell strain. The surviving DHFR-positive cells were selected in αMEM without ribonucleosides and deoxyribonucleosides with 10% FCS. Highly producible cells were then selected by addition of methotrexate (MTX) to the medium. The concentration was increased stepwise from 0.0025 μM, to 0.05 μM, and finally to 1 μM, to obtain highly producible cells.[12]

After reaching confluence, the culture medium was replaced by serum-free αMEM and the medium was collected every 2 days, nine times. The collected medium was centrifuged at 6000 rpm at 4°C for 15 minutes, filtered, and stored at 4°C until the large-scale purification procedures.

Preparation of Anti-REF-1/TFPI-2 Antibody and ELISA

Peptide antibody for REF-1/TFPI-2 was generated, using peptide NH_2-SGGCHRNRIENRFPDE-COOH, corresponding to residues 106-120 as an antigen. Rabbit antiserum was purified on a protein A column (Prosep A; Amersham Biosciences). A sandwich ELISA system was constructed by using primary antibody (5 μg/mL) generated against whole REF-1 protein, biotinylated secondary peptide antibody (5.2 μg/mL) raised against amino acids 106 through 120, and the avidin HRP anti-rabbit antibody. During the process of REF-1 purification, protein quantification was determined by this ELISA kit with detection sensitivity of 10 ng/mL.

Purification of CHO Cell–Derived Recombinant REF-1/TFPI-2

Forty liters of culture supernatant was applied to a gel filtration column (S-Sepharose FF, 5 × 15 cm, 300 mL; Amersham Biosciences) at 2.4 L/h and the column was washed with 1.2 L of 20 mM sodium citrate buffer (pH 5.0) and 1.7 L of buffer containing 0.2 M NaCl. Protein was eluted by 20 mM sodium citrate (pH 5.0)/0.4 M NaCl. TFA was added to the eluate at a final concentration of 0.1% and further purified by reverse-phase chromatography (Resource RPC column, 0.46 × 10 cm, 3 mL; Amersham Biosciences). The elution was performed with acetonitrile gradient of 0% to 70% in 0.1% TFA (pH 2.0). REF-1 was eluted in 19 mL of 31% to 35% acetonitrile fraction. This fraction was diluted with 40 mM PBS (pH 7.2) to twofold volume and applied to a gel filtration column (SP-Sepharose FF, 1 × 1.3 cm, 1 mL; Amersham Biosciences). REF-1 was eluted with 20 mM PBS (pH 7.2) containing 0.45 M NaCl.

Determination of Protease Inhibitor Activity

Plasmin inhibition by REF-1 was analyzed by a method introduced previously.[13] Reaction buffer (50 mM Tris-HCl [pH 7.5], 5 mM $CaCl_2$, 0.1 M NaCl, 0.01% Tween 20) was added to 96-well plastic plates followed by the addition of 0.4 μg aprotinin (Boehringer-Yamanouchi, Tokyo, Japan) and REF-1/TFPI-2 at final concentration of 5 μg/mL. One hundred twenty-five nanograms of plasmin was added (Chromogenix, Milano, Italy) and incubated at room temperature for 30 minutes. Fifty microliters of substrate S-2251 (Val-Leu-Lys-pNA, 1 mg/mL; Chromogenix) was added and the absorbance was measured at 405 to 450 nm for 15 minutes with a microplate photometer (UV/Visible Spectrometer DU640; Beckman Coulter, Fullerton, CA) every 20 seconds. The percentage of relative activity in the inhibitor concentration was then calculated.

Determination of RPE Cell Production of Cytokines

The relationship between RPE cell growth and production of the growth factor bFGF, transforming growth factor (TGF)-β1, transforming growth factor (TGF)-β2, epidermal growth factor (EGF), granulocyte colony-stimulating factor (G-CSF), granulocyte-macrophage CSF (GM-CSF), and macrophage-CSF (M-CSF), and the cytokines interleukin (IL)-1α, IL-6, IL-8, tumor necrosis factor (TNF)-α by human primary RPE cells was examined. The cells were grown in DMEM with 15% FCS for 3 days and the medium then replaced by serum-free DMEM. The cytokines in the culture supernatant were determined for two additional days by ELISA kits (Amersham International, Buckinghamshire, UK; R&D Systems, Minneapolis, MN; Immuno-Biological Laboratories, Gunma, Japan).

Western Blot Analysis of REF-1 for RPE Cell Extract

Cellular extract was obtained from RPE cells by using M-PER (Pierce, Rockford, IL) detergent mixture. A sample amount of 7.2 μg was

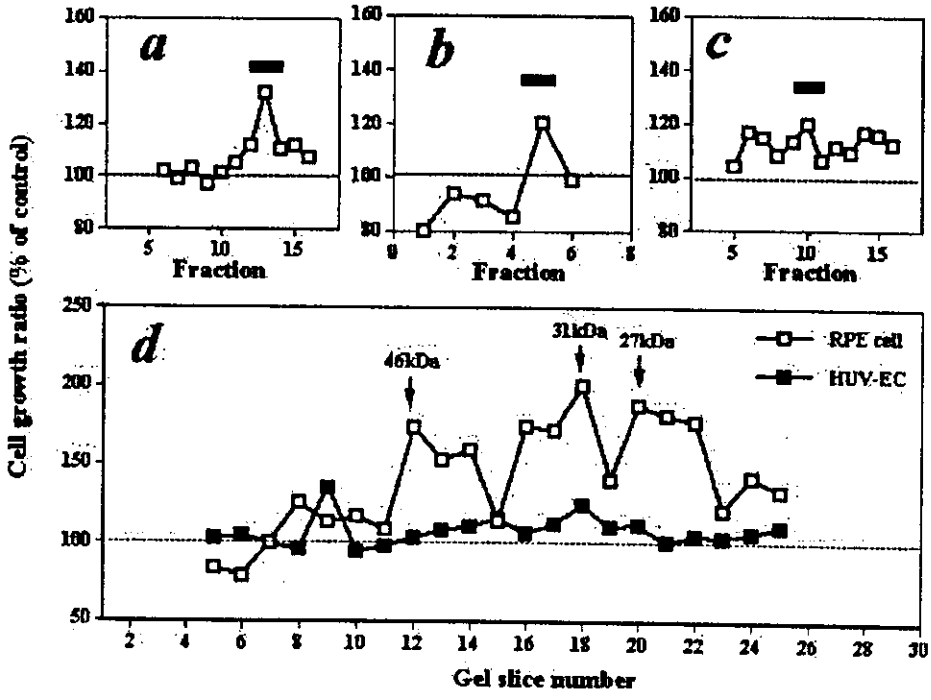

FIGURE 2. Chromatography was used to determine RPE cell growth-promoting activity. Profiles of the activity on S-Sepharose (a), polypropyl-A (b), and Vydac-C4 (c) columns and on a nonreducing SDS-PAGE gel (d). Data denote active fractions collected. In the SDS-PAGE fraction, the growth-promoting activity was examined in RPE cells and HUVECs.

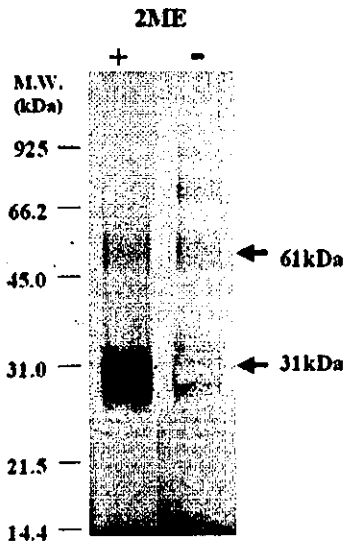

FIGURE 3. SDS-PAGE pattern of the RPE cell growth-promoting factor REF-1 isolated from the conditioned medium of human fibroblasts. Approximately 1 μg/lane of the purified protein was loaded and made visible with silver staining after electrophoresis under reducing (+2ME) and nonreducing (−2ME) conditions. A major band at 31 kDa and a minor band at 61 kDa correspond to the monomeric and dimeric forms of REF-1, respectively.

applied to each lane in 12% polyacrylamide gels. For positive control, bacteria expressing REF-1 protein was added (see Fig. 7, lane 4). After the separation, proteins were transferred to a nitrocellulose membrane (Schleicher & Schuell, Rellichausen, Germany), blocked for 1 hour with the blocking solution containing 10% milk diluent-blocking solution (KPL, Gaithersburg, MD) and 0.1% Tween-20 in phosphate-buffered saline (pH 7.4). The membrane was probed with a rabbit polyclonal anti-REF-1 antibody (1 μg/mL). The specific signal was detected by incubation of anti-rabbit IgG HRP secondary antibody (New England BioLabs, Beverly, MA) followed by chemiluminescence reactions with luminol reagent A and peroxide reagent B, as recommended by the manufacturer (New England BioLabs) and made visible with a chemiluminescence imager (Lumi-Imager F1; Roche Applied Science, Tokyo, Japan).

RNA Isolation from RPE cells and RT-PCR of REF-1

Total RNA was isolated from cultured fourth-passage human primary RPE cells with a total RNA isolation kit (RNA-Bee-RNA Isolation Reagent; Tel-Test, Friendswood, TX). Total RNA samples were digested by RNase-free DNase (Roche Diagnostics Japan) to minimize the risk of genomic DNA contamination. First-strand cDNA was synthesized using random primers (SuperScript First-Strand Synthesis System for RT-PCR; Invitrogen Japan). PCR was performed using 1 μg of single-strand cDNA with 2.5U *Taq* DNA polymerase in a volume of 50 μL. After predenaturation at 95°C for 5 minutes, 30 cycles were performed, including denaturation at 95°C for 30 seconds, annealing at 65°C for 30 seconds, and extension at 72°C for 1 minute, followed by 1% agarose gel electrophoresis. The primers used were: 5′-ATTCTGCTGCTTTTC-CTGAC-3′ (sense primer) and 5′-CAGCTCTGCGTGTACCTGTC-3′ (antisense primer).

RESULTS

Isolation and Identification of an RPE Cell Growth–Promoting Factor

The RPE cell growth-promoting fraction was purified from 100 L of starting material to 0.5 mL of SDS-PAGE gel extract. REF-1 was concentrated by 2×10^5-fold after the final step of purification. The profile of the RPE cell growth-promoting factor is shown at each step in Figure 2. The peak of RPE cell growth promotion was mainly detected in three fractions of molecular mass 46 ± 3, 31 ± 3, and 27 ± 3 kDa on the SDS-PAGE gel. The 31-kDa fraction had the highest RPE cell growth-promoting effect. This fraction showed very low growth stimulation in HUVECs for all molecular sizes detected. The 31-kDa active fraction was separated from the SDS-PAGE gel under reducing–nonreducing conditions. The 31-kDa band was made visible as a major component by silver staining (Fig. 3). There was a minor component at 61 kDa that was predicted as a dimeric form of REF-1. Amino-terminal sequence analysis was performed on the purified 31-kDa protein.

Amino-Terminal Sequence of RPE Cell Growth–Promoting Factor

Amino-terminal sequence analysis of the 31-kDa component resulted in the following sequence: NH_2-Asp-Ala-Glu-Gln-Pro-Thr-Gly-Thr-Asn-Ala-Glu-Ile-Xaa-Ala-COOH (14 amino acids).

In addition, amino-terminal sequence analysis of the 27-kDa component gave nine residues of sequences identical with the 31-kDa component. The polypeptide was named REF-1. Because the amino-terminal sequence of REF-1 was apparently identical with TFPI-2^{28}-PP5,[9] molecular cloning of REF-1 was performed to confirm the whole sequence of the 31-kDa protein. For the 46-kDa active component isolated on SDS-PAGE gel, the amino acid sequence could not be identified because of insufficient quantity of the protein.

Molecular Cloning of REF-1

Although REF-1 was identical with TFPI-2 at the amino-terminal, molecular cloning was performed to determine the complete cDNA of REF-1. One of the 16 clones isolated had an amino-terminal sequence identical with that of TFPI-2. The cloned REF-1 molecule consisted of 235 amino acids, and the theoretical molecular mass of this polypeptide was 27 kDa. The position of three tandemly arranged Kunitz-type domains and two binding sites of predicted asparagine-linked sugar chains were identical with TFPI-2. From the available evidence, we concluded that REF-1 is identical with TFPI-2. The calculated molecular mass increased by 4 to 6 kDa after possible glycosylation to molecular mass between 31 and 33 kDa.

TABLE 1. Purification of CHO-Cell-Derived Recombinant REF-1

Purification Step	Volume (mL)	Protein Conc (μg/mL)	Total Protein (mg)	REF-1 (mg)	Yield (%)	Purity (%)	Purification (×)
CHO cell CM	40,000.0	113.8	4552.0	10.8	100	0.24	1
S-Sepharose	800.0	82.8	66.2	8.6	80	13.00	54
Resouce RPC	40.0	159.0	6.4	6.4	59	87.00	360
SP-Sepharose	4.2	913.0	3.8	3.8	35	97.00	400

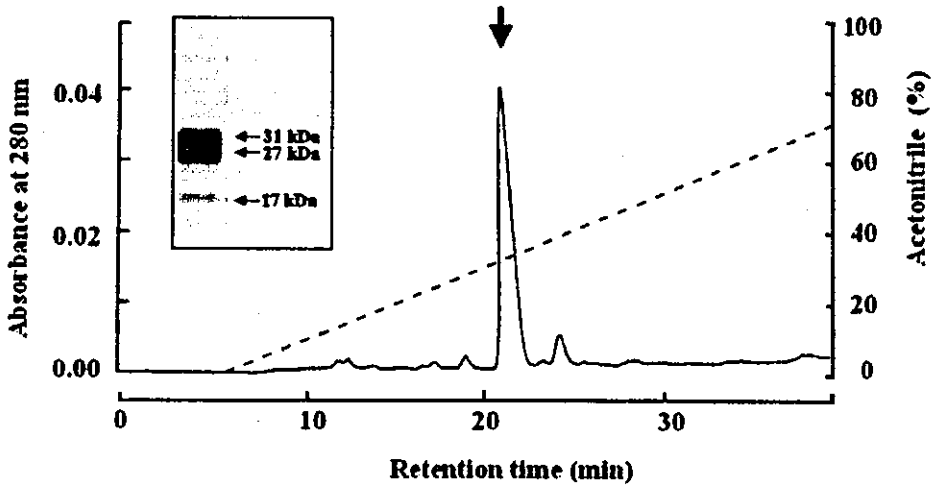

FIGURE 4. Reverse-phase chromatographic profile of CHO-cell-derived recombinant REF-1 in a final purification step. SDS-PAGE was used to amplify recombinant REF-1. Approximately 5 μg of the purified protein was loaded and made visible with Coomassie blue R-250 staining after electrophoresis under reducing (+2ME) conditions. Major components at 31 and 27 kDa and a minor component at 17 kDa were observed.

Purification of CHO Cell–Derived Recombinant REF-1

We developed a large-scale purification procedure for CHO cell-derived recombinant REF-1. From 40 L of conditioned medium of recombinant REF-1-CHO cells, recombinant REF-1 was purified by the combination of cation exchange chromatography and reverse-phase high-performance liquid chromatography (HPLC) as shown in Table 1. The purity of the final recombinant REF-1 was more than 97% on SDS-PAGE gel and was free of pyrogen. The reverse-phase HPLC profile and SDS-PAGE pattern of purified CHO cell-derived recombinant REF-1 are shown in Figure 4.

Molecular Heterogeneity of REF-1

A molecular heterogeneity of the CHO-cell-derived recombinant REF-1 was observed. Three forms of REF-1 at molecular masses of 31 ± 1, 27 ± 1, and 17 ± 1 kDa were found. The ratios for each size were approximately 40% for 31 kDa, 50% for 27 kDa, and 10% for 17 kDa. The 31- and 27-kDa components were major and appeared to be different because of attached sugar chains. The 17-kDa component was smaller than the theoretical molecular mass by approximately 10 kDa. This form was possibly produced by extracellular protease digestion after the secretion of the mature form based on the amino acid composition analysis. The molecular mass of 10 kDa was calculated to match the 28-kDa component lacking the C-terminal portion.

Currently, data are not available for the differences in biological effects of the different molecular forms. TFPI-2 also demonstrated molecular heterogeneity of 31 and 27 kDa, and it has been suggested that this may be due to different glycosylated forms.[14]

Cell Growth–Promoting Activity of Recombinant REF-1

The growth-promoting activity of REF-1 in K-1034 cells was dose dependent, with a bell-shaped curve (Fig. 5a), perhaps because of the downregulation of receptor at a higher REF-1 concentration.

The growth-promoting activities of other relevant cytokines, TFPI-1, CNTF, and bFGF on RPE cells were compared at a 10-ng/mL concentration. TFPI-1 is a member of the TFPI family with 35% amino acid sequence homology with TFPI-2; however, RPE cells did not respond to TFPI-1. CNTF, a human ciliary nerve nutritional factor, also did not stimulate RPE cell proliferation. However, the growth stimulation of bFGF was stronger than that of REF-1 (Fig. 5b).

Growth stimulation of HUVECs, human fibroblasts, rabbit primary RPE cells, and fourth-passage human primary RPE cells was also examined (Fig. 5c). A 12% and 25% increase after

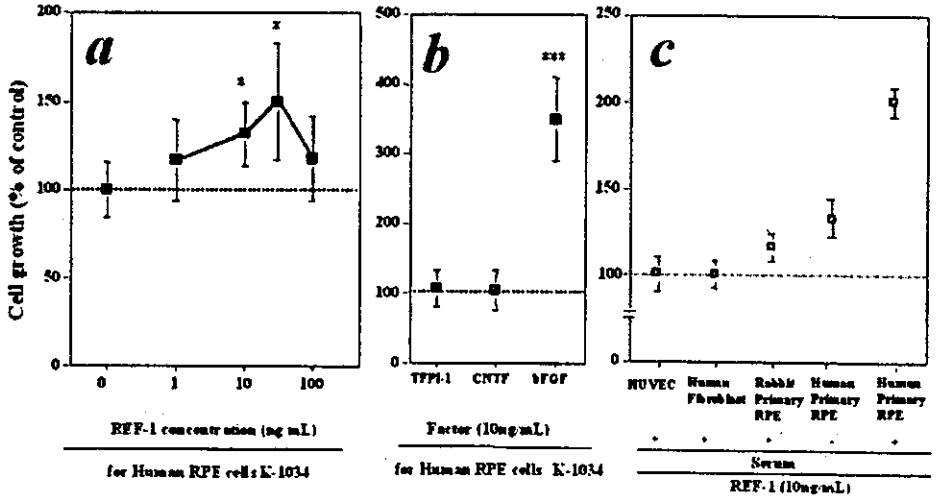

FIGURE 5. Cell proliferation activity of recombinant REF-1. Dose-dependent REF-1 activity in human K-1034 RPE cells (a), growth-promoting activities of TFPI-1, CNTF, and bFGF in human K-1034 RPE cells (b), and proliferative response of HUVECs, human fibroblast, rabbit primary RPE cells, and human primary RPE cells to 10 ng/mL REF-1 (c).

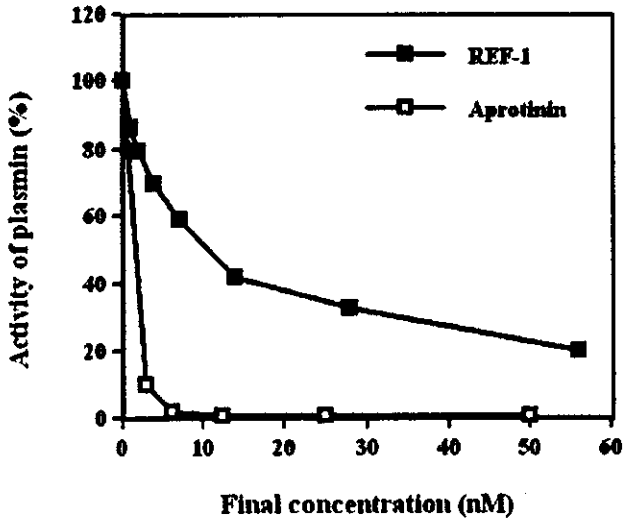

FIGURE 6. Protease inhibitory activity of REF-1. The residual activities of plasmin with aprotinin (positive control, 4 μg/mL) or REF-1/TFPI-2 (5 μg/mL) were determined, in 96-well plastic plates, with S-2251 (Val-Leu-Lys-pNA, 1 mg/mL) used as a substrate. The percentage of relative activity in the inhibitor concentration was calculated from absorbance at 405 to 450 nm.

stimulation by REF-1 was observed in rabbit primary RPE cells and human primary RPE cells, respectively. Significant proliferation was observed in human primary RPE cells cultured in medium with 15% FCS.

Proteinase Inhibitory Activity

REF-1 inhibited plasmin (Fig. 6), and it was confirmed that it inhibited serine protease.

Determination of REF-1 in Human Primary RPE Cells

The existence of REF-1 was determined in human primary RPE cells by Western blot analysis and RT-PCR (Fig. 7). REF-1 was not detected in RPE cells by Western blot under the conditions we used; however, REF-1 mRNA was detected in total RNA extracted from human primary RPE cells by 30 cycles of PCR.

Effect of REF-1 Treatment on Cytokine Production of RPE Cells

Eleven cytokines and growth factors were measured in serum-free culture medium of fourth-passage human primary RPE cells treated with 10 ng/mL of REF-1 for 2 days. TGF-β1 and GM-CSF were significantly induced by 4.7- and 2.4-fold, respectively. bFGF, IL-6, IL-8, and M-CSF showed no or only a moderate increase with REF-1 treatment. TGF-β2, IL-1β, G-CSF, TNF-α, and EGF were undetectable (Table 2).

Discussion

We have isolated and identified a biologically active protein that stimulated RPE cell to proliferate and consider it to be a potential therapeutic agent. This factor has growth-promoting properties that it exerts on RPE cells and was identified as REF-1 protein. Molecular cloning showed that this factor was homologous to the TFPI-2/PP5 protein. The RPE cell growth-promoting effect of REF-1/TFPI-2 was found to be more specific to RPE cells than to fibroblasts and HUVECs. Currently, there are no reports of factors that specifically stimulate the growth of RPE cells, although several growth factors such as bFGF, EGF, PDGF, and VEGF are growth promoters. These factors also have other properties, such as angiogenesis and potential stimulation of endothelial cell growth and can cause proliferative vitreoretinopathy by fibroblast proliferation. These undesirable properties do not allow them to be used for the treatment of retinal diseases. Although REF-1/TFPI-2 has a relatively weaker growth-promoting action than bFGF in vitro, it did not stimulate endothelial cell growth or fibroblast proliferation. Thus, the specificity of REF-1/TFPI-2 to RPE cells is greater than that of other growth factors (Fig. 5).

We determined the growth-promoting activity of REF-1/TFPI-2 using 10th- to 20th-passage human K-1034 RPE cells, primary HUVECs, primary rabbit RPE cells, and 4th-passage primary human RPE cells. Early-passage RPE cells responded

Determination of REF-1 in RPE Cells by Western Blotting Analysis and RT-PCR

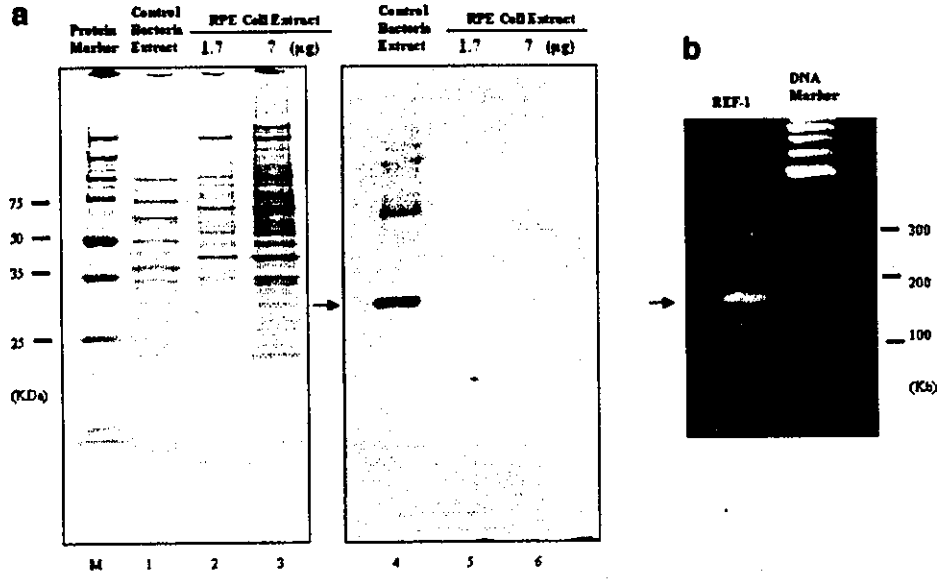

FIGURE 7. Determination of REF-1 in human primary RPE cells. REF-1 in human primary RPE cells was determined by Western blot analysis or RT-PCR. (a) Western blot of REF-1 for human primary RPE cell extract. *Lane 1*: Coomassie staining of bacteria extract expressing recombinant REF-1 (34 kDa); *lane 2*: Coomassie staining of human RPE cell extract (1.7 μg); *lane 3*: Coomassie staining of RPE cell extract (7 μg); *lane 4*: Western blot of bacteria extract expressing recombinant REF-1 (34 kDa); *lane 5*: Western blot of RPE cell extract (1.7 μg); *lane 6*: Western blot of RPE cell extract (7 μg). (b) RT-PCR of REF-1 transcript in total RNA extracted from human primary RPE cells. A single band was observed after 30 cycles of amplification.

TABLE 2. Production of Cytokines by Human Primary RPE Cells Treated with REF-1 (10 ng/mL)

Cytokine	REF-1 (pg/10^5 cells)		
	−	+	+/−
bFGF	508	546	1.0
TGF-β1	673	3163	4.7
TGF-β2	Nondetectable	Nondetectable	—
IL-1β	Nondetectable	Nondetectable	—
IL-6	1770	1922	1.1
IL-8	556	837	1.5
G-CSF	Nondetectable	Nondetectable	—
GM-CSF	817	1959	2.4
M-CSF	420	509	1.2
TNF-α	Nondetectable	Nondetectable	—
EGF	Nondetectable	Nondetectable	—

satisfactorily to REF-1; however, aged K-1034 RPE cells did not (data not shown), whereas primary rabbit RPE cells and primary HUVECs responded poorly to REF-1. Aged K-1034 RPE cells retained their response to basic FGF as well as early-passaged cells. These observations indicate that the growth-promoting effect of RPE-1 may be age-related and that it probably stimulates growth by a pathway different from that used by other growth factors such as bFGF. Although, growth stimulation was observed for human primary RPE cells in both serum-free and serum-added medium, REF-1 favored the latter condition, resulting in fourfold proliferation. Exogenous factor(s) may be involved in this effect.

Our experiments showed that at least 2 of 11 cytokines were stimulated by REF-1 treatment. To our surprise, TGF-β1 production was significantly induced (4.7-fold) in REF-1-treated compared with nontreated cells. A possible explanation for this phenomenon is that TGF-β1 production is stimulated to suppress and balance the rapid growth rate of RPE cells. This suggestion may be supported by the inhibitory effect of TGF-β1 on RPE cell proliferation.[21]

Another cytokine, increased by 2.4-fold, was colony-stimulating factor GM-CSF. GM-CSF is known to be an important regulator of macrophage, granulocyte, dendritic cell, and eosinophil behavior.[22,23] RPE cells have properties similar to macrophages—that is, to phagocytose and generate different cytokines, including GM-CSF.[24] In RPE cells, GM-CSF has been reported to be upregulated in response to TNF-α,[24] IL-1α,[25] or IL-1β[26] and downregulated by IFN-γ.[26] The signal transduction mechanism for upregulation of GM-CSF by REF-1 is currently under investigation.

REF-1 was detected by RT-PCR in human primary RPE cells after 30 cycles of PCR; however, Western blot analysis failed to detect REF-1 in the experimental conditions we used. REF-1 mRNA may require specific stimulation to produce protein in RPE cells.

TFPI-2 has been shown to act as an anticoagulant[8] and serine protease inhibitor.[9] It is unclear whether these activities are correlated with growth promotion. Recent studies on TFPI-2 have shown that it has novel biological effects, such as inhibition of matrix metalloproteinase (MMP),[15,16] promotion of smooth muscle growth,[17] and modulation of melanoma and glioma invasion.[18,19] The relationship between these activities and promotion of RPE cell proliferation is still unknown. TFPI-2/REF-1 has been found in human ciliary epithelium[20] and may play an important role in the normal RPE environment. It also has potential for therapeutic use for ocular tissue damage. To confirm these possibilities further pharmacological evaluations in vivo are needed, using suitable animal models and effective drug delivery methods to the damaged sites.

References

1. Marmor MF. Introduction to structure, function, and diseases of the retinal pigment epithelium. In: Marmor MF, Wolfensberger TJ. *The Retinal Pigment Epithelium: Function and Disease*. London, UK: Oxford University Press. 1998;3–12.
2. Hackett SF, Schoenfeld CL, Freund J, Gottsch JD, Bhargave S, Campochiaro PA. Neurotrophic factors, cytokines and stress increase expression of basic fibroblast growth factor in retinal pigmented epithelial cells. *Exp Eye Res*. 1997;64:865–873.
3. Campochiaro PA, Glaser BM. Platelet-derived growth factor is chemotactic for human retinal pigment epithelial cells. *Arch Ophthalmol*. 1985;103:576–579.
4. Kaven CW, Spraul CW, Zavazava NK, Lang GK, Lang GE. Growth factor combinations modulate human retinal pigment epithelial cell proliferation. *Curr Eye Res*. 2000;20:480–487.
5. Schweigerer L, Neufeld G, Friedman J, Abraham JA, Fiddes JC, Gospodarowicz D. Capillary endothelial cells express basic fibroblast growth factor, a mitogen that promotes their own growth. *Nature*. 1987;325:257–259.
6. Cassidy L, Barry P, Shaw C, Duffy J, Kennedy S. Platelet derived growth factor and fibroblast growth factor basic levels in the vitreous of patients with vitreoretinal disorders. *Br J Ophthalmol*. 1998;82:181–185.
7. Kliffen M, Sharma HS, Mooy CM, Kerkvliet S, de Jong PT. Increased expression of angiogenic growth factors in age-related maculopathy. *Br J Ophthalmol*. 1997;81:154–162.
8. Sprecher CA, Kisiel W, Mathewes S, Foster DC. Molecular cloning, expression, and partial characterization of a second human tissue-factor-pathway inhibitor. *Proc Natl Acad USA*. 1994;91:3353–3357.
9. Miyagi Y, Koshikawa N, Yasumitsu H, et al. cDNA cloning and mRNA expression of a serine proteinase inhibitor secreted by cancer cells: identification as placental protein 5 and tissue factor pathway inhibitor-2. *J Biochem*. 1994; 116:939–942.
10. Utsumi J, Iizuka M, Kobayashi S. Interferon production with multitray culture system on a large scale. *J Interferon Res*. 1984;4:9–16.
11. Kigasawa K, Soushi S, Tanaka Y, Obazawa H. Morphologic and chromosomal study of a human retinal pigment epithelial cell line. *Jpn J Ophthalmol*. 1994;38:10–15.
12. Sano E, Okano K, Sawada R, et al. Constitutive long-term production and characterization of recombinant human interferon-gammas from two different mammalian cells. *Cell Struct Funct*. 1988; 13:143–159.
13. Petersen LC, Sprecher CA, Foster DC, Blumberg H, Hamamoto T, Kisiel W. Inhibitory properties of a novel human Kunitz-type protease inhibitor homologous to tissue factor pathway inhibitor. *Biochemistry*. 1996;35:266–272.
14. Rao CN, Reddy P, Liu Y, et al. Extracellular matrix-associated serine protease inhibitors (Mr. 33, 000, 31.000, and 27, 000) are single-gene products with differential glycosylation: cDNA cloning of the 33-kDa inhibitor reveals its identity to tissue factor pathway inhibitor-2. *Arch Biochem Biophys*. 1996;335:82–92.
15. Rao CN, Mohanam S, Puppala A, Rao JS. Regulation of proMMP-1 and ProMMP-3 activation by tissue factor pathway inhibitor-2/matrix-associated serine protease inhibitor. *Biochem Biophys Res Commun*. 1999;255:94–98.
16. Herman MP, Sukhova GK, Kiesiel W, et al. Tissue factor pathway inhibitor-2 is a novel inhibitor of matrix metalloproteinases with implication for atherosclerosis. *J Clin Invest*. 2000;107:1117–1126.
17. Shinoda E, Yui Y, Hattori R, et al. Tissue factor pathway inhibitor-2 is a novel mitogen for vascular smooth muscle cells. *J Biol Chem*. 1999;274:5379–5384.
18. Konduri SD, Tasiou A, Chandrasekar N, Nicolson GL, Rao JS. Role of tissue factor pathway inhibitor-2 (TFPI-2) in amelanotic melanoma (C-32) invasion. *Clin Exp Metastasis*. 2000;18:303–308.
19. Konuri SD, Rao CN, Chandrasekar N, et al. A novel function of tissue factor pathway inhibitor-2 (TFPI-2) in human glioma invasion. *Oncogene*. 2001;20:6938–6945.

20. Ortego J, Escribano J, Coca-Prados M. Gene expression of proteases and protease inhibitors in the human ciliary epithelium and ODM-2 cells. *Exp Eye Res.* 1997;65:289–299.
21. Lee SC, Seong GJ, Kim SH, Kwon OW. Synthesized TGF-beta s in RPE regulates cellular proliferation. *Kor J Ophthalmol.* 1999;13:16–24.
22. Gasson JC, Molecular physiology of granulocyte-macrophages colony stimulating factors. *Blood.* 1991;77:1131–1145.
23. Fischer HG, Frosch S, Reske K, Reske-Kunz AB. Granulocyte-macrophages colony-stimulating factor activates macrophages derived from bone marrow cultures to synthesis of MHC class II molecules and to augmented antigen presentation. *J Immunol.* 1988;141: 3882–3888.
24. Crane IJ, Kuppner MC, McKillop-Smith S, Wallace CA, Forrester JV. Cytokine regulation of granulocyte-macrophage colony-stimulating factor (GM-CSF) production by human retinal pigment epithelial cells. *Clin Exp Immunol.* 1999;115:288–293.
25. Plank SR, Huang X-N, Robertson JE, Rosenbaum JT. Retinal pigment epithelial cells produce interleukin-1β and granulocyte-macrophage colony-stimulating factor in response to interleukin-1α. *Curr Eye Res.* 1993;12:205–212.
26. Crane IJ, Wallace CA, Forrester JV. Regulation of granulocyte-macrophage colony-stimulating factor in human retinal pigment epithelial cells by IL-1β and IFN-γ. *Cell Immunol.* 2001;209:132–139.

Analysis of Porcine Optineurin and Myocilin Expression in Trabecular Meshwork Cells and Astrocytes from Optic Nerve Head

Minoru Obazawa,[1,2] *Yukihiko Mashima,*[2] *Naoko Sanuki,*[1] *Setsuko Noda,*[3] *Jun Kudoh,*[4] *Nobuyoshi Shimizu,*[4] *Yoshihisa Oguchi,*[2] *Yasuhiko Tanaka,*[1] *and Takeshi Iwata*[1]

Purpose. To determine the cDNA sequences and analyze the expression of porcine optineurin and myocilin in trabecular meshwork cells (TMCs) and astrocytes from the optic nerve head under normal and experimental conditions.

Methods. Both porcine optineurin and myocilin were cloned to determine the cDNA sequences. Porcine TMCs and astrocytes were isolated and treated with dexamethasone (500 nM) for 2 weeks, incubated under hypoxic conditions (7% O_2) for 72 hours, or exposed to 33 mm Hg hydrostatic pressure for 72 hours. A 10% mechanical stretch for 24 hours was also performed on TMCs. The expression level of the optineurin and myocilin transcripts was analyzed by real-time quantitative PCR.

Results. The sequences of porcine optineurin and myocilin cDNA were determined, and the expression of both genes was confirmed in both TMCs and astrocytes. Amino acid sequences of porcine optineurin and myocilin were homologous to those of humans by 84% and 82%, respectively, and shared protein motifs and modification sites. The expression of myocilin mRNA by TMCs and astrocytes was increased by 8.0- and 5.5-fold, respectively, after exposure to dexamethasone. In contrast, the expression of optineurin was suppressed to 68% in TMCs and 48% in astrocytes after exposure to dexamethasone. A significant reduction of myocilin expression was observed after 72 hours of incubation under hypoxic conditions in both types of cells, whereas optineurin was not affected. Hydrostatic pressure for 72 hours and mechanical stretching for 24 hours had minimal affects on gene expression of both optineurin and myocilin.

Conclusions. The high homology of porcine optineurin and myocilin to the comparable human genes indicates that pigs can be used to study changes in gene expression in hypertensive eyes. The alterations in expression of myocilin but not of optineurin under stress suggest that different mechanisms in the phenotype of glaucoma associated with the two genes are involved in development of glaucoma. (*Invest Ophthalmol Vis Sci.* 2004;45:2652-2659) DOI:10.1167/iovs.03-0572

Characteristic degeneration and excavation of the optic nerve head are found in glaucomatous eyes. These changes are considered to be due to ocular hypertension with the intraocular pressure (IOP) continuously more than 21 mm Hg. In contrast, there are patients with normal ocular tension who show glaucomatous changes in the optic nerve head. These patients, in whom there is no evidence of an elevation of IOP at any time, are said to have normal-tension glaucoma (NTG).

Currently three genes—myocilin (*MYOC*),[1,2] cytochrome P4501B1 (*CYP1B1*),[3,4] and optineurin (*OPTN*)[5]—are associated with glaucoma. Optineurin is the most recent gene to be identified and is responsible for 16.7% of families with hereditary NTG.[5] It has been identified and studied by different groups under various names: NRP, NF-κB essential modulator (NEMO)-related protein[6]; FIP-2, adenovirus E3-14-kDa interacting protein 2[7]; Huntingtin interacting protein L (HYPL)[8]; and transcription factor IIIA interacting protein (TFIIIA-INTP).[9] Optineurin is homologous to NEMO, a structural and regulatory subunit of the high molecular weight kinase complex (IKK) that is responsible for the phosphorylation of NF-κB inhibitors.[6]

Some of the functions of optineurin are known. They include inhibition of the tumor necrosis factor (TNF)-α pathway,[7] interaction with transcription factor IIIA,[9] and mediation of the interaction of Huntingtin and Rab8 for regulation of membrane trafficking and cellular morphogenesis.[8] Optineurin is induced by TNF-α and binds to an inhibitor of TNF-α and the E3-14.7-kDa protein.[7]

The optineurin protein contains two leucine zippers (LZs); an N-terminal LZ responsible for the association with Rab8, and a C-terminal LZ required for Huntingtin. The gene is mapped to 10p14 and contains 16 exons encoding a 66-kDa protein. It contains two putative bZIP transcription factor motifs, a C2H2 type zinc finger, and two LZ domains.

Recently, Vittitow and Borrás[10] reported that elevated IOP, and exposure to TNF-α and dexamethasone (DEX) led to an upregulation of optineurin expression in an organ culture system. However, it is still unclear how mutations of the optineurin gene lead to glaucoma.

Another gene associated with glaucoma is myocilin, which is found in 36% of juvenile-onset POAG and 4% of adult-onset POAG.[11-15] Myocilin is a 57-kDa protein that contains motifs homologous to the olfactomedin domain where nearly all mutations in patients with POAG have been identified.[1,11-15]

Pigs and miniature pigs are readily available and have been used for a wide variety of medical studies, including tissue transplantation.[16,17] Because their eyes are similar in size and

From the [1]National Institute of Sensory Organs, National Tokyo Medical Center, Tokyo, Japan; the Departments of [2]Ophthalmology and [4]Molecular Biology, Keio University School of Medicine, Tokyo, Japan; and the [3]Department of Nursing, School of Health Science, Tokai University, Isehara, Kanagawa, Japan.

Supported by Research on Eye and Ear Sciences from the Ministry of Health, Labor, and Welfare, Japan; a grant for Scientific Research and Exploratory Research from the Ministry of Education, Science, Sports, and Culture of Japan; and funding from the Research for the Future Program from the Japan Society for the Promotion of Science.

Submitted for publication June 7, 2003; revised December 1, 2003; accepted December 8, 2003.

Disclosure: **M. Obazawa**, None; **Y. Mashima**, None; **N. Sanuki**, None; **S. Noda**, None; **J. Kudoh**, None; **N. Shimizu**, None; **Y. Oguchi**, None; **Y. Tanaka**, None; **T. Iwata**, None

The publication costs of this article were defrayed in part by page charge payment. This article must therefore be marked "*advertisement*" in accordance with 18 U.S.C. §1734 solely to indicate this fact.

Corresponding author: Takeshi Iwata, Laboratory of Cellular and Molecular Biology, National Institute of Sensory Organs, National Tokyo Medical Center, 2-5-1, Higashigaoka, Meguro, Tokyo 152-8902, Japan; iwatatakeshi@kankakuki.go.jp.

Investigative Ophthalmology & Visual Science, August 2004, Vol. 45, No. 8

anatomy to human eyes,[18] pigs have often been used to study the aqueous outflow system and the regulation of IOP.

The purpose of this study was to clone both the porcine optineurin and myocilin genes to determine their cDNA sequences, and then to use the sequences to determine the transcriptional response of isolated porcine trabecular meshwork cells (TMCs) and astrocytes from the optic nerve head after exposure to dexamethasone (DEX), increased hydrostatic pressure, hypoxia, and mechanical stretching.

Materials and Methods

Cell Cultures

Pig eyes were obtained within 3 hours of death from a local abattoir. The eyes were disinfected in 0.2% povidone iodine for 10 minutes followed by soaking in 70% alcohol for 30 seconds. The eyes were washed several times in phosphate-buffered saline (PBS) and cut into halves along the equator.

After the lens and iris were removed from the anterior half, the trabecular tissue was trimmed from the cornea at the Schwalbe's line and then from the sclera, as described.[19,20] The optic nerve head was separated from the sclera and surrounding tissues. The prelaminar region was dissected from the optic nerve head and cut into three or four pieces.[21,22] The trabecular and prelaminar tissues were placed separately in 35-mm plastic Petri dishes in Dulbecco's modified Eagle's medium (DMEM; Invitrogen-Gibco, Grand Island, NY) with 10% fetal bovine serum (Sigma-Aldrich, St. Louis, MO) and 1% antibiotic-antimycotic (Invitrogen-Gibco).

The tissues were incubated for 1 to 2 weeks at 37°C in humidified 5% CO_2 and 95% air until cells migrated from the tissue onto the surface of the culture dish. Cells were isolated, and fourth-passage cells were obtained for experimental use. The cells that migrated from the optic nerve head were confirmed to be astrocytes by immunostaining with anti-glial fibrillary acidic protein (GFAP), a protein marker for astrocytes (Sigma-Aldrich).

Cloning of Porcine Optineurin cDNA

mRNA was isolated from cultured TMCs using mRNA isolation kits (MicroPoly(A)Pure; Ambion, St. Austin, TX). Primers (sense primer, 5′-ATGTCCCATCAACCTCTGAGCT-3′, antisense primer 5′-TGTCCTCGGCTCCTCTTTGAAA-3′) were designed to include the conserved sequences for human, mouse (Discovery System; Celera, Gaithersburg, MD), and rat to amplify the open reading frame of porcine optineurin mRNA using a commercial system (Superscript One-Step RT-PCR System; Invitrogen-Gibco), according to the manufacturer's protocol.

The PCR products were cloned into a TA cloning vector (pDrive; Qiagen, Valencia, CA) using a PCR Cloning Kit (Qiagen), and the inserts were sequenced using a fluorescent dideoxynucleotide automated sequencer (CEQ2000XL DNA Analysis System; Beckman-Coulter, Fullerton, CA). The missing 3′ and 5′ ends of the cDNAs were amplified using the 3′ and 5′ rapid amplification of cDNA ends (RACE) method (Marathon cDNA Amplification Kit; BD Biosciences-Clontech, Palo Alto, CA). The full-length cDNA sequence of porcine optineurin can be obtained from GenBank under accession number AF513722 (http://www.ncbi.nlm.nih.gov/Genbank; provided in the public domain by the National Center for Biotechnology Information, Bethesda, MD).

Cloning of Porcine Myocilin cDNA

The same mRNA used for optineurin cDNA cloning was used for myocilin cDNA amplification. The sense primer, 5′-ATGCCAGCTS(G/C)TCCAGCTGCT-3′, and antisense primer, 5′-GACCATGTTGAAGTTGTCCCA-3′, were designed to include the conserved sequence of human, mouse, rat, and bovine myocilin and to amplify the open reading frame of porcine myocilin mRNA, using the RT-PCR system (Superscript One-Step RT-PCR System; Invitrogen-Gibco). The PCR products were cloned into a TA cloning vector (TA Cloning Kit; Invitrogen, San Diego, CA), and the inserts were sequenced. The missing 3′ and 5′ ends of the cDNA were amplified using the RACE method (Marathon cDNA Amplification Kit; BD Biosciences-Clontech). The full-length cDNA sequence of porcine myocilin can be obtained from GenBank under accession number AF350447.

Sequence Analysis of Porcine Optineurin and Myocilin

Amino acid sequences of both optineurin and myocilin were analyzed for domain structure and potential protein modification sites. The PROSITE scanning tool[23] (http://www.nhri.org.tw/prosite/; provided in the public domain by the Swiss Institute of Bioinformatics, Geneva, Switzerland) was used to scan the optineurin protein sequence for the occurrence of patterns and profiles stored in the PROSITE database. Potential glycosylation and phosphorylation sites were predicted by the program developed by Hansen et al.,[24] and Blom et al.,[25] respectively. Sequence homology was determined by a sequence-analysis program (Omiga 2.0; Accelrys, San Diego, CA).

Stress Experiments for Optineurin and Myocilin

All stress experiments were performed using fourth-passage TMCs and astrocytes from three different porcine eyes. For the DEX treatment, DEX stock solution (50 mM DEX/dimethyl sulfoxide) was added to cultured TMCs and astrocytes at a final concentration of 500 nM. The culture medium was replaced every 3 days and maintained for 2 weeks. For control, cultured cells were treated with dimethyl sulfoxide alone.

To examine the effect of hypoxia, both types of cultured cells were incubated in 7.0% O_2 and 5% CO_2, in a multiple gas incubator (model 9200; Wakenyaku, Kyoto, Japan) for 12, 24, 48, or 72 hours. Control cells were incubated for the same times in 5% CO_2 and 95% air in a standard CO_2 incubator.

To examine the effects of hydrostatic pressure, we exposed both types of cultured cells to a hydrostatic pressure of 33 mm Hg above atmospheric pressure for 12, 24, 48, or 72 hours in a CO_2 incubator, using the system illustrated in Figure 1. The culture flasks were filled with the medium and capped with a silicon stopper to prevent leakage. The height of the reservoir containing the medium was adjusted to control the pressure in the flask. For gas exchange, the medium was circulated with a peristaltic pump (Eyela, Tokyo, Japan), and the pressure was monitored with a pressure gauge (model PG-208; Copal Electronics, Tokyo, Japan). Control cells were exposed to hydrostatic pressure of 3 mm Hg above atmospheric pressure for 12, 24, 48, and 72 hours.

To examine the effects of mechanical stretching, cultured porcine TMCs were transferred onto a 10-cm^2 collagen-coated silicon chamber (S.Tec, Osaka, Japan). The silicon chamber had a 100-μm-thick transparent bottom, and the side walls were 1.5-mm thick to prevent narrowing at the bottom center. The silicon chamber was then attached to a stretching apparatus for a 10% linear stretch for 24 hours in a standard CO_2 incubator. Control cells were plated onto a collagen-coated silicon chamber without the stretching for the same amount of time.

Optineurin and Myocilin Transcript Analysis

Total RNA was isolated from cultured cells exposed to stimuli or stresses (RNAzol B; Tel-Test, Friendswood, TX). The total RNA was reverse transcribed (Superscript First Strand Synthesis System for RT-PCR; Invitrogen-Gibco) according to the manufacturer's protocol. Real-time quantitative PCR was performed to determine the optineurin, myocilin, and glyceraldehyde-3-phosphate dehydrogenase (GAPDH) transcript with a sequence-detection system (GeneAmp 5700; Applied Biosystems, Inc. [ABI], Foster City, CA). PCR reactions were performed in 50 μL of reaction mixture containing 25 μL master PCR mix (SYBR Green PCR Master Mix; ABI), 5 pM primer pairs, and 1 μL cDNA samples. To measure myocilin transcript, 4 μL cDNA samples was used because of lower expression. The 18S ribosomal RNA gene was used as

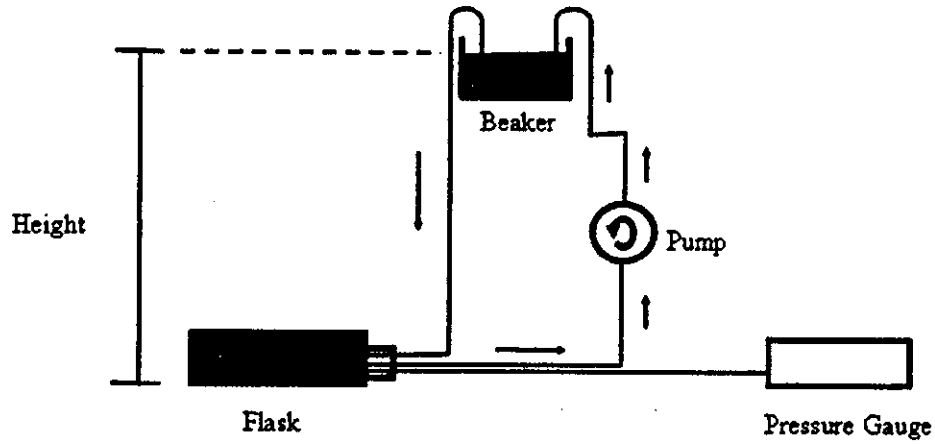

FIGURE 1. System used for hydrostatic pressure experiments. The culture flask was filled with medium and capped with a silicon stopper. The height of the reservoir with the medium was adjusted to maintain the pressure in the flask. For gas exchange, the medium was circulated by a peristaltic pump, and the pressure was monitored with the pressure gauge. For control, cultured cells were exposed to a hydrostatic pressure of 3 mm Hg above atmospheric pressure for 72 hours.

an internal control. All the primers used in these reactions were designed on computer (Primer Express software; ABI). For myocilin cDNA amplification, sense primer 5'-GGTCATTCCGGCAGTGAAGAA-3' and antisense primer 5'-ACGCCGTACTTGCCAGTGATT-3' were used.

For amplification of optineurin cDNA, sense primer 5'-GACCCACAACAGGCTTCTTCA-3' and antisense primer 5'-TCTGCCATTTCCAGCTTTCC-3' were used. For GAPDH cDNA amplification, sense primer 5'-TCATCAGGAATGCCTCCTGTAC-3' and antisense primer 5'-ATGGCATGGACTGTGGTCATG-3' were used. For 18S rRNA, sense primer 5'-GATCGAAGACGATCAGATACC-3' and antisense primer 5'-CCAGACAAATCACTCCACC-3' were used.

To confirm the specificity of PCR reaction, each PCR product was analyzed by agarose gel and subjected to a dissociation curve analysis, according to the manufacturer's instructions.

RESULTS

Cloning of Porcine Optineurin cDNA

The nucleotides and deduced amino acid sequences of porcine optineurin are shown in Figure 2A. A comparison of the predicted amino acid sequences of pig, human, mouse, and rat optineurin is shown in Figure 2B. The porcine optineurin is composed of 574 amino acids, and the homology of porcine optineurin to mouse, rat, and human was 71%, 72%, and 84%, respectively. Two LZ motifs, reported in the human optineurin, were also present in porcine optineurin at residues 143-164 and 437-458 (Fig. 2A, dashed underscore). A glutamic acid-rich region at residues 221-376 (Fig. 2A, solid underscore) and two potential O-glycosylation sites (Fig. 2A, circles) were found. Phosphorylation sites of 20 serine residues, 11 threonine residues, and 1 tyrosine residue were predicted (Fig. 2A, bold italic).

Cloning of the Porcine Myocilin cDNA

The nucleotides and deduced amino acid sequences of porcine myocilin are shown in Figure 3A. A comparison of the predicted amino acid sequences of pig, bovine, mouse, rat, monkey, and human myocilin is shown in Figure 3B. The porcine myocilin is composed of 489 amino acids, which is 14 amino acids shorter at the N terminus and lacks one more amino acid at codon 182 than the human myocilin has. The homology of porcine myocilin to mouse, rat, bovine, monkey, and human was 80%, 79%, 84%, 82%, and 82%, respectively. Porcine myocilin is the smallest myocilin described, and also contained a LZ motif at residues 103-152 (Fig. 3A, dashed underscore). Two predicted N-glycosylation sites and seven O-glycosylation sites were found (Fig. 3A, squares and circles, respectively). Phosphorylation sites of 31 serine residues, 8 threonine residues, and 5 tyrosine residue were predicted (Fig. 3A, bold italic). C-terminal olfactomedin-like domain was more conserved in all species than the N-terminal myosin-like domain.

DEX Treatment

After a 2-week exposure to 500 nM DEX, the expression of optineurin by TMCs and astrocytes was significantly decreased (to 67% and 48%, respectively), compared with that of untreated TMCs and astrocytes (Figs. 4A–C). The expression of porcine myocilin exposed to DEX increased by 8.02 ± 1.26-fold (mean ± SD) and 5.57 ± 1.05-fold in cultured TMCs and astrocytes, respectively. The expression of GAPDH was not altered in both types of cells by exposure to DEX.

Incubation in Hypoxic Conditions

In hypoxic conditions, porcine optineurin was relatively stable at all times points, whereas the expression of porcine myocilin decreased significantly (Figs. 4D–F). The expression of myocilin by astrocytes decreased by an average of 44% after 12 hours and declined to 4% after 72 hours of hypoxia compared with the control. For TMCs, a significant decrease in myocilin expression to 11% was observed after 72 hours compared with that of the control. We did not observe any cell death of both types of cells histologically at all time points (Fig. 5).

Incubation under Hydrostatic Pressure and with Mechanical Stretching

After 72 hours under hydrostatic pressure or 24 hours of mechanical stretching, optineurin and myocilin expression was unchanged in both TMCs and astrocytes.

DISCUSSION

Our results demonstrated that both optineurin and myocilin were expressed in porcine TMCs and astrocytes, and their amino acid sequences were homologous to human sequences by 84% and 82%, respectively. The protein motifs and protein modification sites were also shared with humans.

The response of optineurin and myocilin to DEX was different. Optineurin expression was decreased, whereas that of myocilin was increased. The increased expression of myocilin by TMCs confirmed earlier observations,[26–29] but we also detected an increase in astrocytes. Astrocytes are the major glial cells populating the optic nerve head and are probably responsible for the remodeling of the optic nerve head in glaucomatous eyes. Astrocytes are known to function as cellular support

Porcine Optineurin

A

```
ATGTCCCATCAACCTCTGAGCTGCCTGACTGAGAAGGGGGACAGCCCCACCGAAACCACAGGAAATGGACCCCCCACTCTGGCTCACCCAAACCTTGACA   100
M  S  H  Q  P  L  S  C  L  T  E  K  G  D  #  P  (T) E  T  T  G  N  G  P  P  T  L  A  H  P  N  L  D  T
CGTTCACCCCACATGAACTGCTGCAGCAGATGAGAGAGCTTCTAATCGAGAACCATCAGCTGAAAGAAGCCATGAAGCTAAATAATCAAGCTATGAAAGG   200
  F  T  P  H  E  L  L  Q  Q  M  R  E  L  L  I  E  N  H  Q  L  K  E  A  M  K  L  N  N  Q  A  M  K  G
GCGATTTGAGGAGCTTTCAGCCTGGACAGAGAAGCAGAAGGAAGAACGCCTTTTTTTTGAGACCCAGAGCAAAGAAGCCAAAGAGCGCCTAACGGCTCTG   300
 R  F  E  E  L  S  A  W  T  E  K  Q  K  E  E  R  L  F  F  E  T  Q  #  K  E  A  K  E  R  L  T  A  L
AGTCTTGAAAATGAAAAACTGAAGCAAGAACTTGGAAAACTAAAAGGGAAAACTGAAAGGTCATTTGAGGACCTCACTGGGGACCCCAGGGTCCCCAAGG   400
#  L  E  N  E  K  L  K  Q  E  L  G  K  L  K  G  K  T  E  R  #  F  E  D  L  T  G  D  P  R  V  P  K  A
CGGAAGCAGAACAGGAAGTAGAACAGCTGAAGACCCAGGTGGCACGCCTTCAAGCTGAAAAGGCGGATCTGCTGGGCATCGTGTCTGAATTGCAGCTCAA   500
  E  A  E  Q  V  E  V  E  Q  L  K  T  Q  V  A  R  L  Q  A  E  K  A  D  L  L  G  I  V  S  E  L  Q  K
GCTGAACTCAGGTGGCCCCTCTGAAGACTCCTTTGTTGAAATCAGGATGGCTGAGGGAGAAGCAGATGCAGCAATGAAGGAAATCAAGACAAGTCCTGGG   600
 L  N  S  G  G  P  S  E  D  #  F  V  E  I  R  M  A  E  G  E  A  D  A  A  M  K  E  I  K  T  #  P  G
CCCATAAGAACTGATTCCATTGACACGAGCAAATCTGCAGAAGGTACCAGGAATTATTTGGAATTTGAGGAATTAACTGTGAGCCAGCTCCTGCTGTGTC   700
P  I  R  (T) D  #  I  D  T  #  K  #  A  E  G  T  R  N  Y  L  E  F  E  E  L  T  V  S  Q  L  L  L  C  L
TAAGGGAAGGAAACCAGAAGGTGGAGAGACTTGAAATCGCCCTCAAGGAAGCCAAAGAAAGAATTTTAGATTTTGAAAAGAAAGCCAAGGATCGTTCTGA   800
  R  E  G  N  Q  K  V  E  R  L  E  I  A  L  K  E  A  K  E  R  I  L  D  F  E  K  K  A  K  D  R  #  E
GACTGAGACCCAGACAGAAGAGCACAAAGAACAAGAGAAAGAAGAGGAGAAAAGCCCAGAAACTGTTGGAAGTGAAGTGGAAATGTTAAACCTTCAGGTG   900
 T  E  T  Q  T  E  E  H  K  E  Q  E  K  E  E  E  K  #  P  E  T  V  G  #  E  V  E  M  L  N  L  Q  V
ACAACCCTGTTTAAGGAGCTTCAGGAGGCTCACACGAAACTCAGTGAAGCTGAGCTCATGAAGAAGAGACTTCAAGAAAAATGTCAGGCACTTGAAAGGA  1000
T  T  L  F  K  E  L  Q  E  A  H  T  K  L  #  E  A  E  L  M  K  K  R  L  Q  E  K  C  Q  A  L  E  R  K
AAAATTCTGCAACCCCATCAGAGCTGAATGAAAAGCAAGAGCTTCTTTATAATAACAAAAAGTTGGAGCTCCAAGTGGAAAGCATGAGATCAGAAATTAA  1100
  N  #  A  T  P  S  E  L  N  E  K  Q  E  L  L  Y  N  N  K  K  L  E  L  Q  V  E  #  M  R  #  E  I  K
AATGGAGCAAGCCAAAACAGAAGAGGAAAAAGTCCAAATTAACTACTCTACAGTTGACCCACAACAGGCTTCTTCAAGAATACAATAATGCACTGAAAACA  1200
  M  E  Q  A  K  T  E  E  E  K  #  K  L  T  T  L  Q  L  T  H  N  R  L  L  Q  E  Y  N  N  A  L  K  T
ATTGAGGAACTGAAAAGAAGAGAGTCTGAAAAAGTGGATAAGGTGGTGCTGCAGGAACTGAATGGAAAGCTGGAAATGGCAGAGAAGGCCCTGGCTTCCA  1300
I  E  E  L  K  R  R  E  #  E  K  V  D  K  V  V  L  Q  E  L  N  G  K  L  E  M  A  E  K  A  L  A  S  K
AGCAGCTCCAAATGGATGAGATGAAGCAGACCATTGCCAAGCAAGAGAAGGACCTGGAAACCATGGCTGTTCTCAGGGCTCAGATGGAGGTATACTGTTC  1400
  Q  L  Q  M  D  E  M  K  Q  T  I  A  K  Q  E  K  D  L  E  T  M  A  V  L  R  A  Q  M  E  V  Y  C  S
TGACTTTCATGCTGAAAGAGCAGCAAGAGAGAAGATTCATGAAGAAAAGGAGCAACTGGCATTGCAGCTGGCAGTTTTGCTGAAAGACGACAATGCTTTT  1500
 D  F  H  A  E  R  A  A  R  E  K  I  H  E  E  K  E  Q  L  A  L  Q  L  A  V  L  L  K  D  D  N  A  F
GAAGAGGGAGCCAGCAGGCAATCCTTGATGGAAATGCAGAGCCGTCATGGGGCAAGAGCAAGTGATGCTGACCAGCAGGCTTTTCTTGTTCAAAGAGGAG  1600
E  E  G  A  S  R  Q  #  L  M  E  M  Q  S  R  H  G  A  R  A  #  D  A  D  Q  Q  A  F  L  V  Q  R  G  A
CTGAGGATAGAAACTGGCTGCAACAGCAACAACAGAATATTCCAATTCATTCTTGCCCCAAATGTGGAGAAGTTCTGCCTGACATAGATACACTACTGAT  1700
  E  D  R  N  W  L  Q  Q  Q  Q  Q  N  I  P  I  H  S  C  P  K  C  G  E  V  L  P  D  I  D  T  L  L  I
TCACGTTACGGACTGCATCATTTAA                                                                              1800
 H  V  T  D  C  I  I  *
```

B

```
                                                                                                      100
Pig    MSHQPLSCLTEKGDSPTETTGNGPPTLAHPNLDTFTPHELLQQMRELLIENHQLKEAMKLNNQAMKGRFEELSAWTEKQKEERLFFETQSKEAKERLTAL
Mouse  ----------------C-------SNMV--S-----------K---V-----------------------------------N----V----K--
Rat    ----------------SC--P----SNMV----------------K---V-----------------------R-----QL--I---------K--
Human  MSHQPLSCLTEKEDSPSESTGNGPPHLAHPNLDTFTPEELLQQMKELLTENHQLKEAMKLNNQAMKGRFEELSAWTEKQKEERQFFEIQSKEAKERLMAL
                                                                                                      100
                                                                                                      198
Pig    SLENEKLKQELGKLKGKTERSFEDLTGDPRVPKAEAEQEVEQLKTQ              VARLQAEKADLLGIVSELQLKLNSGGPSEDSFVEIRMAEGEA
Mouse  TH---R--E----F-E-S-KPL-----GY-Y-R AL-E---K----VEQEVEHLK IQ-M--R----------------------S----------T---T
Rat    -H---R--E------E-E--P---I--RCGF-RTDL----GATEEAGGAGSGASEDPGE-PSGLR-RT---HS-XTAAQAQLRRLLRRLLRGD--T----
Human  SHENEKLKEELGKLKGKSERSSEDPTDDSRLPRAEAEQEKDQLRTQ              VVRLQAEKADLLGIVSELQLKLNSSGSSEDSFVEIRMAEGEA
                                                                                                      188
                                                                                                      282
Pig    DAAMKEIKTSPGPIRTDSIDTS       KSAEGTRNYLEFEELTVSQLLLCLREGNQKVERLEIALKEAKERILDFEKKAKDRSETETQTEEHKEQEKEE
Mouse  EG----M-NC-T-T---P-SL-       NCT-DA-SCA-------------------------V--R------S------NGH-S--K--ARRADR-- -
Rat    EG----MRN-A--T-----IMG       -CT-DA-TKV-------------------------R------S------NGH-AI-----GSTQKE- -
Human  EGSVKEIKHSPGSTRTVSTGTALSHYRRRSADGAKNYFEHEELTVSQLLLCLREGNQKVERLEVALKEAKERVSDFEKKTSNRSEIETQTEGSTEKENDE
                                                                                                      288
                                                                                                      382
Pig    EKSPETVGSEVEMLNLQVTTLFKELQEAHTKLSEAELMKKRLQEKCQALERKNSATPSELNEKQELLYNNKKLELQVESMRSEIKMEQAKTEEEKSKLTT
Mouse  D-GQ-S--TAPPKD                      WHVPGMSP----------------------V-S-------------------------R-A-
Rat    D-D--S--I---T--V--AS---G-------------------------------------------V-S-W-----------------------R-A-
Human  EKGPETVGSEVEALNLQVTSLFKELQEAHTKLSEAELMKKRLQEKCQALERKNSAIPSELNEKQELVYPNKKLELQVESMLSEIKMEQAKTEDEKSKLTV
                                                                                                      388
                                                                                                      482
Pig    LQLTHNRLLQEYNNALKTIEELKRRESEKVDKVVLQELNGKLEMAEKALASKQLQMDEMKQTIAKQEKDLETMAVLRAQMEVYCSDFHAERAAREKIHEE
Mouse  --A---K----H-K--------TKQQA-----ML----SE---L--Q---------------L----E-------------------------------
Rat    ------K----H-K--R-----TKQQAE-----Q----SE---L--Q-------------------E-------------------------------
Human  LQMTHNKLLQEHNNALKTIEELTRKESEKVDRAVLKELSEKLELAEKALASKQLQMDEMKQTIAKQEEDLETMTILRAQMEVYCSDFHAERAAREKIHEE
                                                                                                      489
                                                                                                  574
Pig    KEQLALQLAVLLKDDNAFEEGASRQSLMEMQSRHGARASDADQQAFLVQRGAEDRNWLQQQQ QNIPIHSCPKCGEVLPDIDTLLIHVTDCII
Mouse  ---------I---EN-DI---G---------C-----T--S---TY-F-------S-QHG--PRSI-----------------Q---M----
Rat    ---------I---EN-D--D-G---------C-----T--S----Y-F----K-MS-QHG--PRS-----------------Q---M----
Human  KEQLALQLAVLLKENDAFEDGG RQSLMEMQSRHGARTSDSDQQAYLVQRGAEDRDWRQQR   NIPIHSCPKCGEVLPDIDTLQIHVMDCII
                                                                                                  577
```

FIGURE 2. Nucleotide sequence and deduced amino acid sequence of porcine optineurin and comparison of porcine optineurin amino acid sequences with those of other species. The coding region is defined by the positions of the initiation codon (ATG) and stop codon (TAA). (A) The porcine optineurin protein is composed of 574 amino acids. *Dashed underscore*: LZ motifs; *solid underscore*: glutamic acid-rich region; *circles*: O-glycosylation sites. (B) Only the amino acids that differ from porcine or human optineurin sequences are shown for mouse and rat. *Hyphens*: the same amino acid residues as human optineurin; *spaces*: the absence of amino acids corresponding to the same location in human optineurin; *asterisks*: positions of amino acids associated with glaucoma.

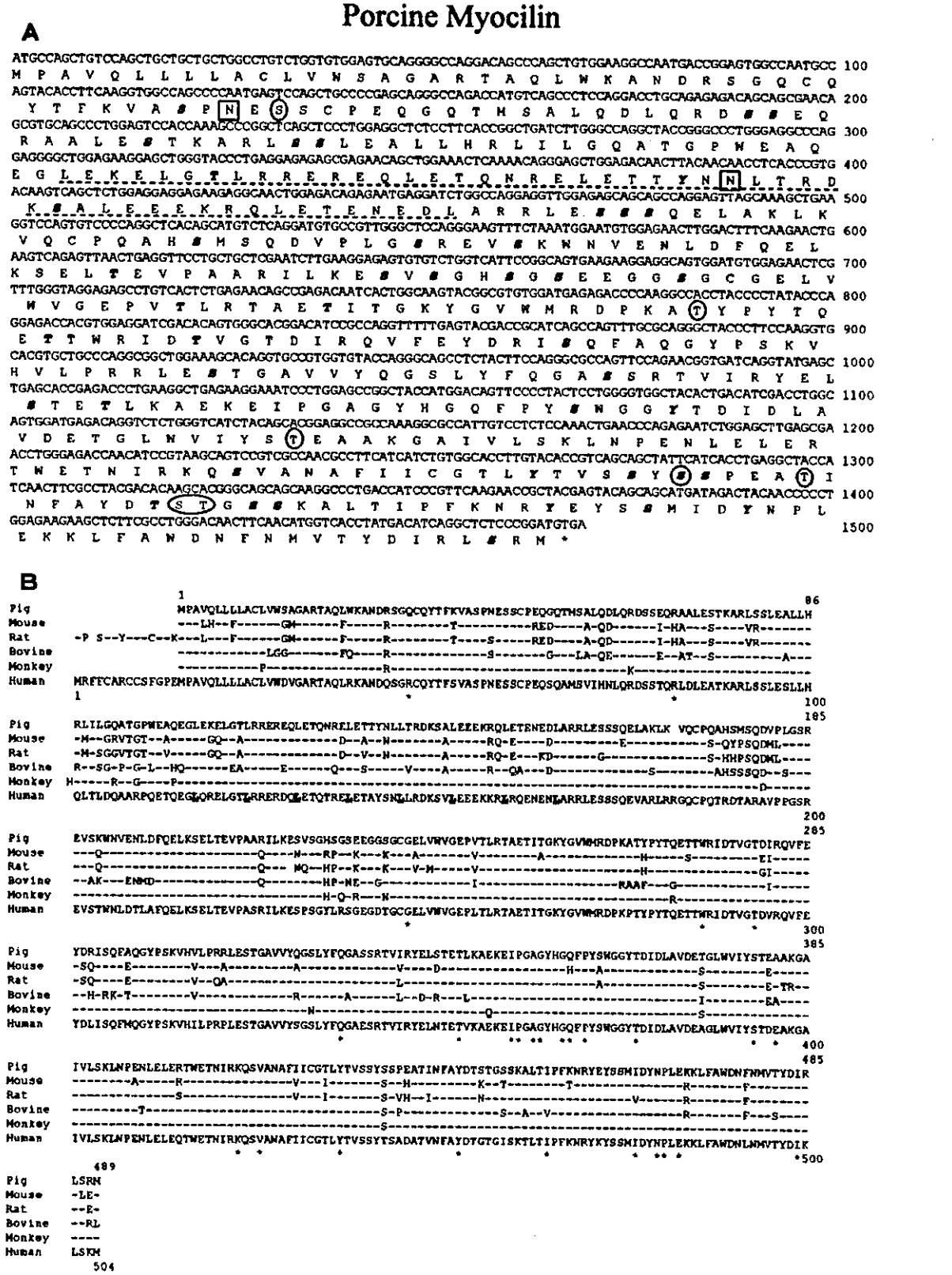

FIGURE 3. Nucleotide sequence and deduced amino acid sequence of porcine myocilin and comparison of porcine myocilin amino acid sequences with those of other species. (**A**) Porcine myocilin is composed of 489 amino acids. *Circles*: O-glycosylation sites; *squares*: predicted N-glycosylation sites; *dashed underscore*: LZ motif. (**B**) Only the amino acids that differ from pig or human myocilin sequence are shown for mouse, rat, bovine, and monkey. *Hyphens*: the same amino acid residues as human myocilin, *spaces*: absence of amino acids corresponding to the same location in human myocilin; *asterisks*: positions of amino acids associated with glaucoma.

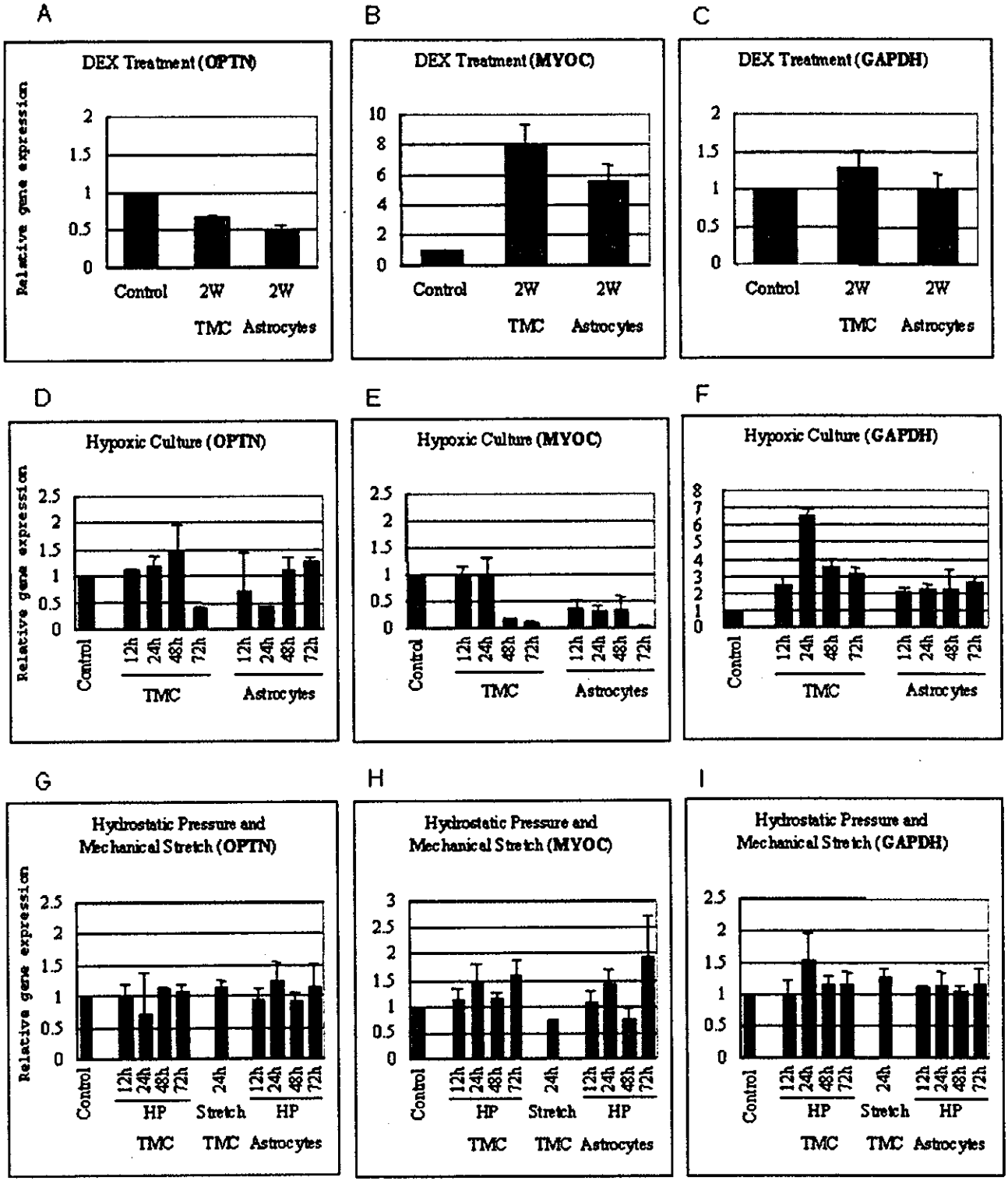

FIGURE 4. Quantitative PCR analysis of optineurin and myocilin under various conditions. The relative gene expression of optineurin, myocilin, and GAPDH is shown for each stimulus or stress condition. Expression level for control cells are shown as 1. (A–C) DEX treatment (500 nM for 2 weeks); (D–F) hypoxia (7.0% O_2); (G–I) hydrostatic pressure (33 mm Hg above atmospheric pressure), and mechanical stretching (a 10% linear stretch for 24 hours).

of the axons as well as synthesizers of various bioactive molecules including extracellular matrix proteins, transforming growth factor (TGF)-β, and platelet-derived growth factor (PDGF) (Tripathi BJ, et al. *IOVS* 1996;37:ARVO Abstract S411; Taylor AW, et al. *IOVS* 1995;36:ARVO Abstract S607; Lambert W, et al. *IOVS* 1997;38:ARVO Abstract S162).[30–33] In the glau-

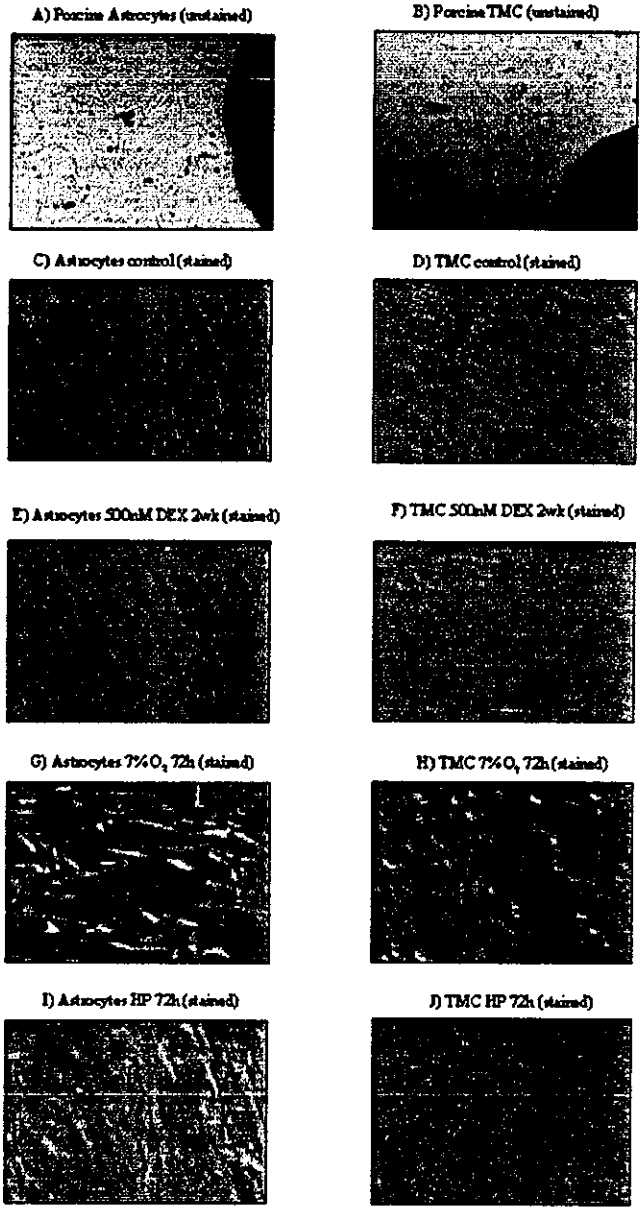

FIGURE 5. Trypan blue staining of TMCs and astrocytes in the various experimental conditions. Trypan blue staining was performed on primary porcine cells to determine cell death caused by stress and stimulation. The stain was added to the culture medium and incubated for 5 minutes before observation. Photographs were taken with a 2-M pixel digital camera (DMC2; Polaroid, Tokyo Japan). (A, B) Unstained primary porcine cells; (C–J) cells stained with TB. *Arrows*: trypan blue–stained dead cells. Magnification, ×100.

comatous process, remodeling of the extracellular matrix and reactive astrocytes induced after mechanical injury by increased IOP may play major roles in damaging the optic nerve axons.[30–33] Significant changes of myocilin expression in astrocytes may alter the normal function of the astrocytes to support the optic nerve head. The tissues in the optic nerve head are central to the pathologic course in glaucomatous eyes; thus, the effect of the fivefold elevation of myocilin transcript after DEX treatment in astrocytes should be further investigated.

Optineurin, in contrast, was significantly decreased in both astrocytes and TMCs after exposure to DEX. Optineurin has been shown to interact with the E3-14.7. kDa protein, one of the three protein encoded by human adenovirus C early region 3 (E3)[7] that use TNF-α or Fas ligand pathways to mediate apoptosis and inflammation. TNF-α plays a critical role in protecting cells from virus infection, which concurrently had been the target for virus. A downregulation of optineurin under DEX may result in the loss of the protective functions, especially in the optic nerve head.

Under hypoxic conditions that mimic the ocular hemodynamic condition in eyes with NTG the expression of myocilin was significantly reduced in both TMCs and astrocytes, whereas the expression of control GAPDH was increased more than twofold after 12 hours in both types of cells. Myocilin transcription was practically shut down in astrocytes after 72 hours, whereas the transcription of optineurin was not affected by the hypoxia. The significant changes of myocilin transcription were not due to cell death, as shown by trypan blue staining (Fig. 5).

A significant increase of GAPDH by hypoxia suggests that the transcriptional machinery is still active in TMCs under hypoxic conditions. In addition, the reduction of both OPTN and MYOC did not occur after 12 hours, which is enough time for the gas exchange in the culture medium of TMCs, suggesting that the transcriptional shut down was not triggered directly by hypoxia but by a factor(s) activated by hypoxia indirectly affecting the transcriptional regulation of both OPTN and MYOC.

Hydrostatic pressure had no affect on gene expression in both TMCs and astrocytes. Recently, Kamphuis and Schneemann[34] also reported no change of optineurin gene expression by pressure elevation in an anterior chamber perfusion model. Pressure elevation in a perfusion system is likely to stress the cells by compression and mechanical stretching. Data collected under our experimental conditions fully agree with the perfusion experiments by Kamphuis and Schneemann.[34] Vittitow and Borrás[10] have reported an increase of optineurin expression by 60% after 7 days of elevated pressure in a perfusion system. Quantification of gene expression by PCR followed by a gel scanner is usually difficult, with an accuracy within 50%, as described.[10] Their results are inconsistent with those of Kamphuis and Schneemann[34] and our results. Our results showed that the expression of myocilin is not affected by hydrostatic pressure or mechanical stretch, although Tamm et al.[27] had previously shown induction of myocilin by mechanical stretching in human TMCs. These results demonstrated that hydrostatic pressure of +33 mm Hg or a mechanical stretch of 10% is not sufficient to increase the myocilin gene expression in TMCs under elevated IOP.

In this study, optineurin and myocilin behaved differently in TMCs from astrocytes during changes of cellular environment by DEX treatment, hypoxia, hydrostatic pressure, or stretching. These results suggest that different mechanisms may be involved in the development of glaucoma by defects in these two genes.

References

1. Stone EM, Fingert JH, Alward WLM, et al. Identification of a gene that causes primary open angle glaucoma. *Science*. 1997;275:668–670.
2. Kubota R, Noda S, Wang Y, et al. A novel myosin-like protein (myocilin) expressed in the connecting cilium of the photoreceptor: molecular cloning, tissue expression, and chromosomal mapping. *Genomics*. 1997;41:360–369.
3. Stoilov I, Akarsu AN, Sarfarazi M. Identification of three different truncating mutations in cytochrome P4501B1 (CYP1B1) as the principal cause of primary congenital glaucoma (Buphthalmos) in families linked to the GLC3A locus on chromosome 2p21. *Hum Mol Genet*. 1997;6:641–647.

4. Stoilov I, Akarsu AN, Alozie I, et al. Sequence analysis and homology modeling suggest that primary congenital glaucoma on 2p21 results from mutations disrupting either the hinge region or the conserved core structures of cytochrome P4501B1. *Am J Hum Genet.* 1998;62:573–584.
5. Rezaie T, Child A, Hitchings R, et al. Adult-onset primary open-angle glaucoma caused by mutations in optineurin. *Science.* 2002; 295:1077–1079.
6. Schwamborn K, Weil R, Courtois G, Whiteside ST, Israel A. Phorbol esters and cytokines regulated the expression of the NEMO-related protein, a molecule involved in a NF-kB-independent pathway. *J Biol Chem.* 2000;275:22780–22789.
7. Li Y, Kang J, Horwitz M. Interaction of an adenovirus E3 14.7-kilodalton protein with a novel tumor necrosis factor alpha-inducible cellular protein containing leucine zipper domains. *Mol Cell Biol.* 1998;18:1601–1610.
8. Hattula K, Peränen J. FIP-2, a coiled-coil protein, links Huntingtin to Rab8 and modulates cellular morphogenesis. *Curr biol.* 2000; 10:1603–1606.
9. Moreland RJ, Dresser ME, Rodgers JS, et al. Identification of a transcription factor IIIA-interacting protein. *Nucleic Acids Res.* 2000;28:1986–1993.
10. Vittitow JL, Borrás T. Expression of optineurin, a glaucoma-linked gene, is influenced by elevated intraocular pressure. *Biochem Biophys Res Commun.* 2002;298:67–74.
11. Adam MF, Belmouden A, Binisti P, et al. Recurrent mutations in a single exon encoding the evolutionarily conserved olfactomedin-homology domain of TIGR in familial open-angle glaucoma. *Hum Mol Genet.* 1997;6:2091–2097.
12. Shimizu S, Lichter PR, Johnson AT, et al. Age-dependent prevalence of mutations at the GLC1A locus in primary open-angle glaucoma. *Am J Ophthalmol.* 2000;130:165–177.
13. Alward WL, Fingert JH, Coote MA, et al. Clinical features associated with mutations in the chromosome 1 open-angle glaucoma gene (GLC1A). *N Engl J Med.* 1998;338:1022–1027.
14. Fingert JH, Heon E, Liebmann JM, et al. Analysis of myocilin mutations in 1703 glaucoma patients from five different populations. *Hum Mol Genet.* 1999;8:899–905.
15. Kubota R, Mashima Y, Ohtake Y, et al. Novel mutations in the myocilin gene in Japanese glaucoma patients: Mutation in Brief (#355). *Hum Mutat.* 2000;16:270.
16. Nielsen TB, Yderstraede KB, Schroder HD, Holst JJ, Brusgaard K, Beck-Nielsen H. Functional and immunohistochemical evaluation of porcine neonatal islet-like cell clusters. *Cell Transplant.* 2003; 12:13–25.
17. Fujiki Y, Fukawa K, Kameyama K, et al. Successful multilineage engraftment of human cord blood cells in pigs after in utero transplantation. *Transplantation.* 2003;75:916–922.
18. McManamin PG, Steptoe RJ. Normal anatomy of the aqueous humor outflow system in the domestic pig eye. *J Anat.* 1991;178: 65–77.
19. Borisuth NSC, Tripathi BJ, Tripathi RC. Identification and partial characterization of TGF-beta 1 receptors on trabecular cells. *Invest Ophthalmol Vis Sci.* 1992;33:596–603.
20. Okada Y, Matsuo T, Ohtsuki H. Bovine trabecular cells produce TIMP-1 and MMP-2 in response to mechanical stretching. *Jpn J Ophthalmol.* 1998;42:90–94.
21. Yang JL, Neufeld AH, Zorn MB, Hernandez MR. Collagen type I mRNA levels in cultured human lamina cribrosa cells: effects of elevated hydrostatic pressure. *Exp Eye Res.* 1993;56:567–574.
22. Hernandez MR, Igoe F, Neufeld AH. Cell culture of the human lamina cribrosa. *Invest Ophthalmol Vis Sci.* 1988;29:78–89.
23. Gattiker A, Gasteiger E, Bairoch A. ScanProsite: a reference implementation of a PROSITE scanning tool. *Appl Bioinf.* 2002;1:107–108.
24. Hansen JE, Lund O, Tolstrup N, Gooley AA, Williams KL, Brunak S. NetOglyc: Prediction of mucin type O-glycosylation sites based on sequence context and surface accessibility. *Glycoconj J.* 1998;15: 115–130.
25. Blom N, Gammeltoft S, Brunak S. Sequence- and structure-based prediction of eukaryotic protein phosphorylation sites. *J Mol Biol.* 1999;294:1351–1362.
26. Clark AF, Steely HT, Dickerson JE Jr, et al. Glucocorticoid induction of the glaucoma gene myocilin in human and monkey trabecular meshwork cells and tissues. *Invest Ophthalmol Vis Sci.* 2001; 42:1769–1780.
27. Tamm ER, Russell P, Epstein DL, Johnson DH, Piatigorsky J. Modulation of myocilin/TIGR expression in human trabecular meshwork. *Invest Ophthalmol Vis Sci.* 1999;40:2577–2582.
28. Polansky JR, Fauss DJ, Chen P, et al. Cellular pharmacology and molecular biology of the trabecular meshwork inducible glucocorticoid response (TIGR) gene product. *Ophthalmologica.* 1997; 211:126–139.
29. Taniguchi F, Suzuki Y, Kurihara H, et al. Molecular cloning of the bovine myocilin and induction of its expression in trabecular meshwork cells. *Invest Ophthalmol Vis Sci.* 2000;41:2070–2075.
30. Hernandez MR, Janethe DO, Pena MD. The optic nerve head in glaucomatous optic neuropathy. *Arch Ophthalmol.* 1997;115: 389–395.
31. Radius RL. Anatomy of the optic nerve head and glaucomatous optic neuropathy. *Surv Ophthalmol.* 1987;32:35–44.
32. Varela HJ, Hernandez MR. Astrocyte responses in human optic nerve head with primary open-angle glaucoma. *J Glaucoma.* 1997; 6:303–313.
33. Fukuchi T, Ueda J, Hanyu T, Abe H, Sawaguchi S. Changes in transforming growth factor-beta and platelet-derived growth factor in the optic nerve head in monkey experimental glaucoma. *J Jpn Ophthalmol Soc.* 1999;103:193–200.
34. Kamphuis W, Schneemann A. Optineurin gene expression level in human trabecular meshwork does not change in response to pressure elevation. *Ophthalmic Res.* 2003;35:93–96.

Journal of Dermatological Science (2004) 35, 221–223

ELSEVIER

www.intl.elsevierhealth.com/journals/jods

LETTER TO THE EDITOR

The MICA5.1 allele is not associated with susceptibility to effects of ultraviolet-B radiation on induction of contact hypersensitivity

Acute low-dose ultraviolet radiation (UVR) impairs the induction of contact hypersensitivity (CH) when hapten is epicutaneously applied to the exposed site [1]. This outcome occurs only in certain inbred strains of mice, referred to as UVB-susceptible (UVB-S) mice [1]. In these mice, with susceptibility alleles at the *Tlr4* and *Tnfa* loci, UVR prevents CH induction through a process that requires the intracutaneous tumor necrosis factor (TNF)-α [1]. In humans, approximately half of the normal, healthy volunteers represent the UVB-S phenotype [2]. It was reported that the human TNF locus, which is identical to that of mice, was associated with the UVB phenotype in human subjects, this implied that a susceptible locus, which determined the UVB phenotype, was identical in mice and humans [3].

The gene product of the major histocompatibility complex (MHC) class I chain-related gene A (MICA) is a cell stress-induced glycoprotein that is expressed in epithelial cell lines, gastrointestinal epithelia, freshly isolated keratinocytes, and monocytes. Although the role of MICA has not been completely elucidated, its reaction with γδ T and natural killer (NK) cells suggests an association with tumor rejection [4]. The insertion polymorphism of nucleotide G in the transmembrane region of MICA, namely MICA5.1 (or MICA*0801 according to WHO nomenclature), is characterized by a frame-shift mutation leading to a premature intradomain stop codon; thus, denying the molecule of its 42 aa cytoplasmic tail [5]. In polarized epithelial cells, although the full-length MICA protein is sorted to the basolateral membrane, the gene product of the MICA5.1 allele is aberrantly transported to the apical surface [5]. The physiological location of MICA within epithelial cells is governed by its cytoplasmic tail, implying that impairment in MICA5.1 homozygous individuals may be relevant to the immunological surveillance exerted by NK and T lymphocytes on epithelial malignancies. Since the UVB phenotype is associated with the occurrence of skin cancers [1], we determined whether the MICA5.1 allele was associated with the UVB phenotype.

Normal Caucasoid volunteers were enrolled for these studies, as previously described [2]. All participants gave informed consent and the local committee of Ethics for Clinical Investigation approved of the study.

The method used for delivering UVB light to buttock skin has previously been described in detail [2]. Briefly, all subjects were exposed to 144 mJ/cm^2 of UVB light per day for four consecutive days. Induction of CH was achieved with 2000 μg dinitrochlorobenzene (DNCB) [2]. This dose was carefully applied to irradiated buttock skin within 1 h of the fourth UVB treatment (on day 0). On day 30, elicitation of CH was accomplished by painting 50 μg DNCB on the ventral surface of the forearm. The cutaneous responses were clinically assessed 2, 4, and 7 days thereafter, according to the scoring method described earlier [2]. Individuals who exhibited contact dermatitis were designated as UVB-R, while the other individuals were designated as UVB-S.

The genomic DNA samples used in this study were obtained from 24 individuals who were ascertained as belonging to the UVB phenotype. We failed to amplify DNA from 2 samples that were taken from individuals enrolled in a previous study, probably due to a lack of DNA in the samples [2]. We also used 6 DNA samples (3 samples carrying the MICA5.1 allele) from the 10th International Histocompatibility Workshop.

The insertion polymorphism at position 959 of the *MICA* gene was defined by a polymerase chain reaction-restriction fragment length polymorphism (PCR-RFLP) technique developed in our laboratory. Briefly, primers were designed to yield a 98 bp product; 5′ primer (MICA5.1F), 5′-CAT GTT TCT GCT GTT GCT GCC G-3′, and a 3′ primer (MICA5.1R), 5′-CTG GAC CCT CTG CAG CTG A-3′. These complemented areas at positions 937–958 and 1029–1047 of the *MICA* gene [6,7]. A single nucleotide substitution at position 957 (see above; underlined) was included in the forward primer to generate an *Hpa*II

0923-1811/$30.00
doi:10.1016/j.jdermsci.2004.06.005

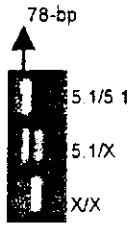

Fig. 1 Detection of the MICA5.1 allele. The PCR products were treated with *Hpa*II. A 98 bp fragment was detected solely in the MICA5.1-positive samples (5.1). Fragments other than the 98 bp fragment were detected when samples had alleles other than MICA5.1 (X). Samples were assigned as MICA5.1 positive when the MICA5.1 specific fragments (78 bp) were detected following cleavage of samples with *Hpa*II. Detection of SNP (insertion of G at position 959) was validated in the various HLA-homozygous cell lines with and without the MICA5.1 allele.

restriction endonuclease site (CCGG) in after the insertion of G at position 959 (solely in the MICA5.1 allele). Genomic DNA was amplified in 25 μl of reaction mixture, as described previously [2,3]. The cycling conditions were as follows: following preincubation at 94 °C for 1 min, 40 cycles at 94 °C for 0.5 min, 50 °C for 0.5 min and 72 °C for 0.5 min. Following a 3 h digestion with *Hpa*II (New England Biolabs, MA, USA), the alleles were separated by electrophoresis using a 3% agarose gel, and subsequently visualized by ethidium bromide staining. The presence of nucleotide G at position 959 (*Hpa*II site) was suggested by the presence of two 78 and 20 bp digestion products (Fig. 1).

The differences in allele distribution and allele frequency amongst each group were examined for statistical significance by application of the Chi-square (χ^2) test. The probability (P) values of <0.05 were considered significant. Two-loci associations were calculated by the 2×2 contingency table analysis [2].

First, we examined single nucleotide polymorphisms (SNPs) typing in the various HLA-homozygous cell lines with and without the MICA5.1 allele. The MICA alleles pertaining to these cell lines have been reported previously [8]. The detection of a fragment pattern was consistent with the expected specificity of the MICA allele that each cell line carried (see figure legend). Fig. 1 shows examples of the detection of MICA5.1-specific fragments. We considered the subjects to be MICA5.1 positive when MICA5.1-specific fragments (78 bp) were detected in samples that were cleaved by the restriction enzyme *Hpa*II.

Table 1 shows the frequency of MICA5.1-positive and -negative samples in UVB-S and UVB-R individuals. There were no differences in the frequency

Table 1 Frequencies of samples with (5.1) and without (X) MICA5.1 allele in the UVB-S and UVB-R groups

	UVB-S (n = 11)		UVB-R (n = 13)	
	N	%	*N*	%
5.1/5.1	2	19	3	23
5.1/X	4	36	6	46
X/X	5	45	4	31

of MICA5.1-positive individuals between the two groups. We checked the association between *HLA-B* and *MICA* alleles because linkage between them has been reported [9]. Individual typing of the HLA-B phenotypes has been previously reported [2]. No associations between HLA-B phenotypes and the MICA5.1 allele were observed in this study (data not shown). We conclude that the *MICA5.1* allele has no association with the susceptibility to the effects of UVR on the induction of CH. Further analysis is currently underway to exclude the *MICA* gene from the susceptible locus of the UVB phenotype associated with the *TNF* region, which is located in an approximate 160-kb interval centromeric of the *MICA* gene. We believe that detection of this SNP by the method developed in this study is simpler and cheaper than detection by direct sequencing, since the length of the nucleotide alignment is dependent on each allele (number of GCT repeats) and nucleotide G at position 959 is located within the (GCT)*n* microsatellite polymorphism in exon 5.

References

[1] Streilein JW, Taylor JR, Vincek V, Kurimoto I, Shimizu T, Tie C, et al. Immune surveillance and sunlight-induced skin cancer. Immunol Today 1994;15:174–9.

[2] Niizeki H, Naruse T, Hecker KH, Taylor JR, Kurimoto I, Shimizu T, et al. Polymorphisms in the tumor necrosis factor (TNF) genes are associated with susceptibility to effects of ultraviolet-B radiation on induction of contact hypersensitivity. Tissue Antigens 2001;58:369–78.

[3] Niizeki H, Inoko H, Wayne Streilein J. Polymorphisms in the TNF region confer susceptibility to UVB-induced impairment of contact hypersensitivity induction in mice and humans. Methods 2002;28:46–54.

[4] Bauer S, Groh V, Wu J, Steinle A, Phillips JH, Lanier LL, et al. Activation of NK cells and T cells by NKG2D, a receptor for stress-inducible MICA. Science 1999;285:727–9.

[5] Suemizu H, Radosavljevic M, Kimura M, Sadahiro S, Yoshimura S, Bahram S, et al. A basolateral sorting motif in the MICA cytoplasmic tail. Proc Natl Acad Sci USA 2002;99:2971–6.

[6] Goto K, Ota M, Ohno S, Mizuki N, Ando H, Katsuyama Y, et al. MICA gene and ankylosing spondylitis: linkage analysis via a transmembrane-encoded triplet repeat polymorphism. Tissue Antigens 1997;49:503–7.